

1

AD-A219 931

DTIC
ELECTE
MAR 29 1990
S D CS D

31 December 1989
POLY-WRI-1571-90

ANNUAL REPORT
on
BASIC RESEARCH IN
ELECTRONICS (JSEP)

CONTRACT NO. F49620-88-C-0075
1 JANUARY 1989 TO 31 DECEMBER 1989

Erich E. Kunhardt
JSEP Principal Investigator
and Program Director

POLYTECHNIC UNIVERSITY
WEBER RESEARCH INSTITUTE
FARMINGDALE, NY 11735

DISTRIBUTION STATEMENT A
Approved for public release;
Distribution Unlimited

90 03 28 091

REPORT DOCUMENTATION PAGE			Form Approved - OMB No. 0704-0188	
<small>Public reporting burden for this collection of information is estimated to average 1 hour per response, including the time for reviewing instructions, searching existing data sources, gathering and maintaining the data needed, and completing and reviewing the collection of information. Send comments regarding this burden estimate or any other aspect of this collection of information, including suggestions for reducing this burden, to Washington Headquarters Services, Directorate for Information Operations and Reports, 1215 Jefferson Davis Highway, Suite 1204, Arlington, VA 22202-4302, and to the Office of Management and Budget, Paperwork Reduction Project (0704-0188), Washington, DC 20503.</small>				
1. AGENCY USE ONLY (Leave blank)		2. REPORT DATE Dec. 31, 1989		3. REPORT TYPE AND DATES COVERED Annual Report 01-01-89 to 12-31-89
4. TITLE AND SUBTITLE BASIC RESEARCH IN ELECTRONICS (JSEP)			5. FUNDING NUMBERS F49620-88-C-0075	
6. AUTHOR(S) E. E. Kunhardt				
7. PERFORMING ORGANIZATION NAME(S) AND ADDRESS(ES) Polytechnic University Weber Research Institute Route 110 Farmingdale, NY 11735			8. PERFORMING ORGANIZATION REPORT NUMBER POLY-WRI-1571-90	
9. SPONSORING/MONITORING AGENCY NAME(S) AND ADDRESS(ES) Air Force Office of Scientific Research/NE Bolling Air Force Base Washington, D. C. 20332			10. SPONSORING/MONITORING AGENCY REPORT NUMBER	
11. SUPPLEMENTARY NOTES				
12a. DISTRIBUTION/AVAILABILITY STATEMENT Approved for public release; distribution unlimited.			12b. DISTRIBUTION CODE	
13. ABSTRACT (Maximum 200 words) This report presents a summary of the scientific progress and accomplishments on research projects in the Joint Services Electronics Program.(JSEP) for the contract period from 1 January 1989 through 31 December 1989. The Joint Services Electronics Program at Polytechnic University is the core of interdisciplinary research in electronics encompassing programs in the Department of Electrical Engineering, Physics, and Chemistry under the aegis of the Weber Research Institute. The research encompassed by this program is grouped under two broad categories: Interactions of Wide-Band Electromagnetic Radiation with Complex Macro- and Micro-Structures (EMI) and Field-Particle Interactions in Matter: Single Particle, Collective and Cooperative Phenomena (FP). The detailed projects (research units) comprising the complete program are listed in the Table of Contents.				
14. SUBJECT TERMS Electromagnetics, microwaves, millimeter waves, waveguides and antennas, optics, solid state interactions and materials.			15. NUMBER OF PAGES 54	
			16. PRICE CODE	
17. SECURITY CLASSIFICATION OF REPORT Unclassified	18. SECURITY CLASSIFICATION OF THIS PAGE Unclassified	19. SECURITY CLASSIFICATION OF ABSTRACT Unclassified	20. LIMITATION OF ABSTRACT	

TABLE OF CONTENTS

Section	Page
Form SF298	
DIRECTOR'S OVERVIEW	i
SIGNIFICANT SCIENTIFIC ACCOMPLISHMENTS	iii
 SECTION I. INTERACTIONS OF WIDE-BAND ELECTROMAGNETIC RADIATION WITH COMPLEX MACRO- AND MICRO-STRUCTURES (EM)	
A. Wide-Band Electromagnetic Wave Interaction With Large Aperture-Coupled Enclosures	1
B. Microparticle Photonics	10
C. Beam-Field Interactions with Nonlinear Thin Films	20
D. Hybrid Methods for Wave Propagation and Scattering	29
E. Optical Switching and Second Harmonic Generation in Nonlinear Thin Films	33
 SECTION II. FIELD-PARTICLE INTERACTIONS IN MATTER (FP)	
A. Nonequilibrium EM Wave-Cooper Pair Interactions in High T_c Superconductors	37

Accession For	
NTIS CRA&I	<input checked="" type="checkbox"/>
DTIC TAB	<input type="checkbox"/>
Unannounced	<input type="checkbox"/>
Justification	
By	
Distribution /	
Availability Codes	
Dist	Avail and or Special
A-1	



DIRECTOR'S OVERVIEW

This report presents a summary of the scientific progress and accomplishments on research projects funded by the Joint Services Electronics Program (JSEP) for the contract period from 1 January 1989 through 31 December 1989. It does not contain information regarding accomplishments on research projects funded in other ways.

The Joint Services Electronics Program at Polytechnic University is the core of interdisciplinary research in electronics conducted by faculty members of the in the Departments of Electrical Engineering, Physics and Chemistry under the aegis of the Weber Research Institute. The Weber Research Institute JSEP Director and Principal Investigator is Professor Erich Kunhardt. He is responsible for the selection of the best individual proposals, coordination between Polytechnic University and the JSEP TCC and coordination between the selected areas of the JSEP Program. In planning the JSEP Program at WRI, a general objective is to develop new projects with 3-6 years of JSEP sponsorship, leading to transition to DoD or other agency program funding. This report covers the second year of our current 3 year cycle. The research encompassed by this program is grouped into two broad categories: Interactions of Wide-Band Electromagnetic Radiation with Complex Macro- and Micro-Structures (EM) and Field-Particle Interactions in Matter: Single Particle, Collective and Cooperative Phenomena (FP). The detailed projects (research units) comprising the complete program are listed in the Table of Contents.

Following our previous practice, Section 2 of every research unit contains a short *summary* of the recent progress. Further details regarding that progress are contained in Section 3, State of the Art and Progress Details.

Each of the research units described in this report is designated, for example, as EM9-1 or FP9-1 corresponding to the category, year (1989) and the number within the category. These numbers follow the number given in our proposal dated 1 July 1987 except that each proposed unit which was phased out in accord with instructions of the TCC has been eliminated and the number of each subsequent project was reduced by one.

It is with sincere regret that we report the following personnel changes on this contract. Professor Gerhard Schaefer passed away on September 17, 1989 after a brief illness. Professor Schaefer is well known for his work on gas lasers and flowing mixture discharges. He will be sorely missed by his colleagues and co-workers. Because of Professor Schaefer's untimely death, and the retirement of Professor Helmut Jurestchke, we have phased out the units in last year's report FP8-1, "Resonant Interactions in Crystals at X-Ray Wavelength" and FP8-2, "Resonances in X-Ray Phonon Interactions in Crystals" and replaced them by units EM9-4 and EM9-5. EM9-4 is an outgrowth of EM8-1, and EM9-5 is experimental work in support of EM8-3.

Following this Overview, we present a *Report on Significant Scientific Accomplishments* which highlights important contributions this year.

REPORT ON SIGNIFICANT ACCOMPLISHMENTS

31 December 1989

Gaussian Beam Algorithm for Radiation from Extended Sources through Complex Layered Media

(L.B. Felsen and J.J. Maciel*)

High frequency propagation from nonfocused or focused extended source distributions through weakly layered materials of relatively arbitrary shape is of interest in a variety of applications and poses wave problems of substantial complexity. Rigorous analytical solutions cannot be found due to the nonseparability, and purely numerical methods, like finite element or finite difference methods, are inefficient or even nonfeasible because of the large problem size in terms of wavelengths. We have developed an entirely new algorithm based on the rigorous decomposition of the incident field into narrow-waisted Gaussian basis beams distributed on a Gabor configuration-wavenumber phase space lattice. The narrow-waisted beams are almost ray-like so that they can be propagated through the layers with a complex (but almost real) ray algorithm, yet they have enough spectral content to avoid the singularities of ray fields near caustic and shadow boundaries. The beam algorithm was found to reconstruct with high precision the exact field -- which can be calculated from a rigorous solution in this prototype problem -- in the near, intermediate, and far zone. The algorithm was then applied to transmission through a circular cylindrical layer, for collimated and strongly focused input fields. No reference solution is available here, but the beam algorithm was subjected to internal self-consistency tests with various choices of basis beams, each being rigorous. The results establish this method as a new and promising means for accurate computation of high frequency wave propagation in complex layered, and possibly also other scattering environments.

* Now at Raytheon Co., Missile Systems Lab., Tewksbury, MA.

SECTION I
INTERACTIONS OF WIDE-BAND ELECTROMAGNETIC RADIATION
WITH COMPLEX MACRO- AND MICRO-STRUCTURES (EM)

A. WIDE-BAND ELECTROMAGNETIC WAVE INTERACTION WITH LARGE APERTURE-COUPLED ENCLOSURES

Prof. L.B. Felsen and G. Vecchi

Unit EM9-1

1. OBJECTIVE(S)

Present technologies relating to communication, surveillance, identification, and other similar tasks demand understanding of the interaction of electromagnetic waves with complex penetrable environments, with the need becoming increasingly more acute for future system development, and with a trend toward wide-band operation in successively higher ranges of frequencies. The environments can be natural (like the earth and its substructure, the troposphere, or the ionosphere) or man-made (like integrated-electronics circuits, aircraft, vehicles or buildings). The objective of this long term research program is to *parametrize* the electromagnetic field in complex environments in terms of "good observables" that can be coordinated with the form of the detected signal. Such a parametrization can then be employed to *predict* the interior-exterior response, to *classify* the environment, and to lay the basis for the *inverse* problem of identification. To achieve this goal, *new analytical techniques* must be developed for coping with *electrically large partially enclosed complex* configurations which have *no* apparent *symmetries*. The problem will be attacked by classifying structural interior and exterior units on the scale of the wavelengths contained in the spectrum of the electromagnetic signal, and exploring the self-consistent dynamic interaction of these units to produce the overall response. *New wave phenomena* - both fundamental (canonical) and interactive, and based on physical phenomenology - will be sought for providing "good" building blocks in the parametrization scheme.

2. STATE OF THE ART

The state of the art in this problem area has been a *piecemeal approach* wherein disconnected strategies have been brought to bear on different parametric regimes. For wavelengths that are larger or at most comparable with the scale of the entire structure, boundary integral equation and T-matrix techniques can attack moderately complex structural shapes, while numerical methods involving finite element and finite difference schemes can model more substantial complexity. The required computational effort is appreciable, and the result, even when numerically reliable, provides no explanation of the wave phenomena that are operative in producing the response.

For shorter wavelengths, the problems become successively "larger" in a computational sense, and overall direct numerical modeling by the above-mentioned and other similar approaches is no longer feasible. One may now attempt to extract global information about the structure by determining its "resonances", which are field patterns (eigenstates) that maintain themselves at

their characteristic resonant frequencies without external excitation. The resonances are undamped for lossless fully enclosed systems (closed cavities) but damped (with complex resonant frequencies) when the structure has access to, or is embedded within, an infinite space. The resonances are broad, and decay rapidly, for low-Q structures (either due to loss or due to strong radiation damping), but can be narrow and highly peaked for high-Q aperture coupled interiors. The most significant and reliably resolvable resonances are those at the lower frequency end where overall dimensions are not substantially larger than the signal wavelength. Thus, the corresponding data processing schemes eliminate the high frequency portion of the signal spectrum. Within the context of transient signal scattering, the resonance approach is known as the singularity expansion method (SEM) because the complex resonances appear as pole singularities in the complex frequency plane; observations (pro and con) pertaining to its implementation for *exterior* problems may be found in the recent literature. Basically, the algorithm requires a good signal to noise ratio, and its ability to resolve structural detail is limited by the inherent *global* nature of the resonances and the concentration on the lower frequency end.

When the wavelengths are small compared not only to the overall extent of the structure but also to structural features (substructures) within the conglomerate, the ray techniques of the geometrical theory of diffraction (GTD), asymptotic techniques associated with physical optics (PO), and related procedures become applicable. These procedures can also be employed for transient analysis near the wavefronts of the impinging signal. However, their implementation so far has been primarily for *exterior* scattering.

The proposed program is *new* because it addresses a class of complex electromagnetic wave interaction problems that has not been explored heretofore. Its implementation requires a thorough understanding of waves and spectra, of asymptotic techniques for localization, of the interrelation between rays, modes, wavefronts, resonances, and other similar "good observable", etc. The groundwork for the new extensions has been laid in our previous pioneering studies of wave phenomena under the JSEP program. Results from these studies have been reported in a large number of publications. References for this background discussion are contained in the last Annual Report (POLY-WRI-1554-89).

3. PROGRESS REPORT

In the last Annual Report (POLY-WRI-1554-89), we have listed three test problems that are presently under investigation:

- A. Complex Resonances of an Open-Ended Plane Parallel Cavity,
- B. Hybrid (Ray-Mode)-(Boundary Element) Method for Wave Scattering from Aperture-Coupled Systems, and

C. Slit-Coupled Convex Perfectly Conducting Thin Cylindrical Shell with Interior Convex Perfectly Conducting Cylindrical Loading.

Problem A was discussed in the last report. In the present report, we deal with Problem C, which involves two-dimensional plane wave scattering from a perfectly conducting thin smoothly convex cylindrical shell, which grants access to a perfectly conducting convex cylindrical interior via a narrow slit aperture (Fig. 1). The incident wave is assumed to be plane, with the magnetic field along the symmetry axis. Both curvature radii are assumed to be slowly varying (with respect to the wavelength), the distance between the two boundaries being moderate and slowly varying.

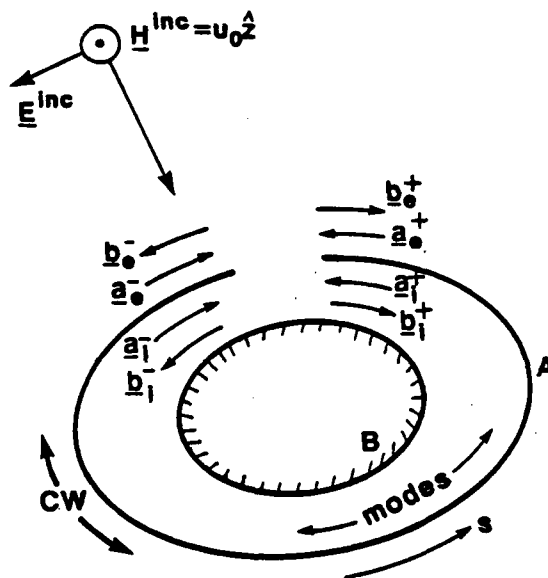


Fig. 1 Geometry of the H-pol scattering problem and state variables

The geometry suggests a parametrization of interior wave phenomena by guided local modes of the nonuniform waveguide formed by the region between the two boundaries, and of exterior wave phenomena by geometrically reflected, slit diffracted and surface guided creeping waves (CW), as described in Sec. 3A.i. The slit produces coupling among the exterior wave types, among the interior wave types, and between the interior and exterior. Section 3A.ii briefly outlines the system of state vectors, propagation matrices and coupling matrices, which render the overall description self-consistent, as described in Sec. 3A.iii. The scattered field is then obtained in Sec. 3A.iv in terms of the self-consistent CW amplitudes. Of special importance is the reduced form in Sec. 3B because it parametrizes the overall complex problem in terms of a simpler problem that is adequate in the regime where internal resonances play a dominant role. In Sec. 3C, the terms representing the incident field excitation and the radiation of self-consistently established waves on the structure are

given a ray parametrization. In Sec. 3D, the field response, when the signal frequency is near one of the resonance frequencies of the internal cavity, is expressed via a resonant mode expansion.

A. Formulation

i. Parametrization

The wavefields in the doubly-connected weakly non-concentric interior region (Fig. 1) are described via the adiabatic (local) azimuthal mode Green's function, which is derived from the concentric annular prototype,

$$G_i(\underline{\rho} | \underline{\rho}') = \sum_{m=-\infty}^{\infty} \Phi_m^i(\rho; s) \Phi_m^i(\rho'; s') \times \frac{e^{ik\tau_m(s, s')}}{2i \sqrt{\mu_m(s) \mu_m(s')}} \quad (1)$$

where the Φ_m^i are radial (transverse) eigenfunctions that depend weakly on the longitudinal coordinate s , and $\mu_m(s)$ are local azimuthal propagation coefficients. The phase function $\tau_m(s)$ is the integral over $\mu_m(s)$.

The exterior description entails the CW wavefields of the conventional geometrical theory of diffraction (GTD).

ii. System Structure

The wavefield amplitudes at the slit are assembled into *state vectors*

$$\underline{A}_\alpha = \begin{bmatrix} a_\alpha^+ \\ a_\alpha^- \end{bmatrix}, \quad \underline{B}_\alpha = \begin{bmatrix} b_\alpha^+ \\ b_\alpha^- \end{bmatrix}, \quad (2)$$

(see Fig. 1) where \pm refers to the left or right sides of the slit, a -type and b -type vectors indicate incident or reflected fields, and the subscripts $\alpha=1, e$ designate internal or external wavespecies. The azimuthal evolution of the state vectors along the smooth portions of the structure is described by propagator matrices obtained from the Green's functions. In the case of interior modes, continuous reflection of adiabatic modes due to varying azimuthal wavenumber may be inserted when needed. System parameters that involve slit scattering and slit coupling are developed from a canonical scattering problem for the local slit geometry [1]. Detailed expressions for all required quantities are being assembled.

iii. Self-Consistent (SC) System for Wave Amplitudes

The system state vector is connected through slit scattering and closed loop propagation, as described by scattering matrices $\underline{S}^i, \underline{S}^e$ (coupling between different wavespecies), and by the propagator matrices $\underline{X}, \underline{P}^e$. The initial amplitudes due to the incident plane wave are expressed through the driving terms \underline{B}_{eg} and \underline{B}_{ig} , representing the wave amplitudes generated by the incident field on a structure *infinitely* extended along the azimuthal direction ("matched" azimuthal transmission lines) (Fig. 2). These relationships yield the self-consistent state equations

$$\begin{cases} \underline{B}_e = \underline{S}^e \underline{A}_e + \underline{S}^{ei} \underline{A}_i + \underline{B}_{eg} \\ \underline{B}_i = \underline{S}^i \underline{A}_i + \underline{S}^{ie} \underline{A}_e + \underline{B}_{ig} \\ \underline{A}_i = \underline{X} \underline{B}_i \\ \underline{A}_e = \underline{P}^e \underline{B}_e \end{cases} \quad (3)$$

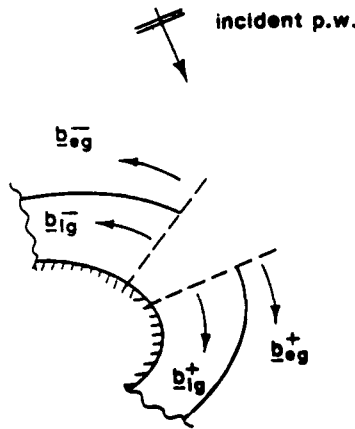


Fig. 2 Driving terms \underline{B}_{ag} . Here and in the following figures, lower case vectors (\underline{b}_{ag}^{\pm}) represent elements in vectors denoted by capital letters, as in (2). $a=e,i$.

iv. Scattered Field

The scattered field may be obtained as a superposition of CW outgoing in both directions with respect to the slit edges (field expansion in the external region), with amplitudes \underline{B}_e at the slit established by the SC system (3),

$$u_s(\rho, s) = \Phi^{eT}(\rho; s) \Pi(s) B_e \quad (4)$$

where $\Phi^e(\rho; s)$ is a vector whose entries are the local radial CW eigenfunctions, the matrix $\Pi(s)$ describes the CW propagation from the slit to the azimuthal location s of the observer, and the superscript T denotes the transposed vector.

B. Resonant Reduced Form

At the high- Q resonances, which are expected for a narrow slit aperture, the interior markedly affects the exterior scattered field. It is then appropriate to load the interior problem with the nonresonant exterior. Elimination of the pair (A_e, B_e) from (3), and then of B_i , and backsubstitution into B_e , allows one to recast (4) as:

$$u_s = u_{res} + u_b \quad (5)$$

where

$$u_{res} = Q^T (1 - X S)^{-1} I_{u_0} \quad (6)$$

is a contribution including all global resonances, expressed by the singularities of $(1 - X S)^{-1}$, with

$$S = X^i + S^{ie} [1 - P^e S^e]^{-1} P^e S^{ei} \quad (7)$$

representing the exterior-loaded internal slit scattering, and with

$$I_{u_0} = X [B_{ig} + S^{ei} (1 - P^e S^e)^{-1} P^e B_{eg}] \quad (8)$$

and

$$Q^T = \Phi^{eT} \Pi [1 - S^e P^e]^{-1} S^{ei} \quad (9)$$

being the global transfer functions from the incident (driving) to the scattered (radiation) field. On the other hand,

$$u_b = \Phi^{eT} \Pi [1 - S^e P^e]^{-1} B_{eg} \quad (10)$$

is a background term containing all wave phenomena that are *not* coupled to the interior, and therefore play no part in the global resonances.

C. Ray (Asymptotic) Parametrization of Driving and Radiation Terms

Driving Term: On use of the equivalence theorem, the terms B_{ag} can be divided into a part B_{ag}^{sh} representing the wave excited in presence of a "shorted" slit (closed shell), plus a part B_{ag}^{sc} due to the radiation of equivalent magnetic currents that account for the slit discontinuity. The currents are determined by an integral equation whose driving term is the field on the closed shell [2].

Background Term: To the leading order of approximation, the slit scattering contribution to u_b in the exterior shadow region of the slit may be expressed via CW geometrical theory of diffraction [3], while in the geometric optical (GO) illuminated region, one has the standard GO reflection.

Radiation Term: The radiation term \underline{Q}^T in (9) due to an internal mode incident on the slit can be divided similarly into a contribution from the direct radiation \underline{D}_{is}^T , in the lit region, and CW diffraction (\underline{L}_d^T) in the shadow region of the shell (Fig. 3).

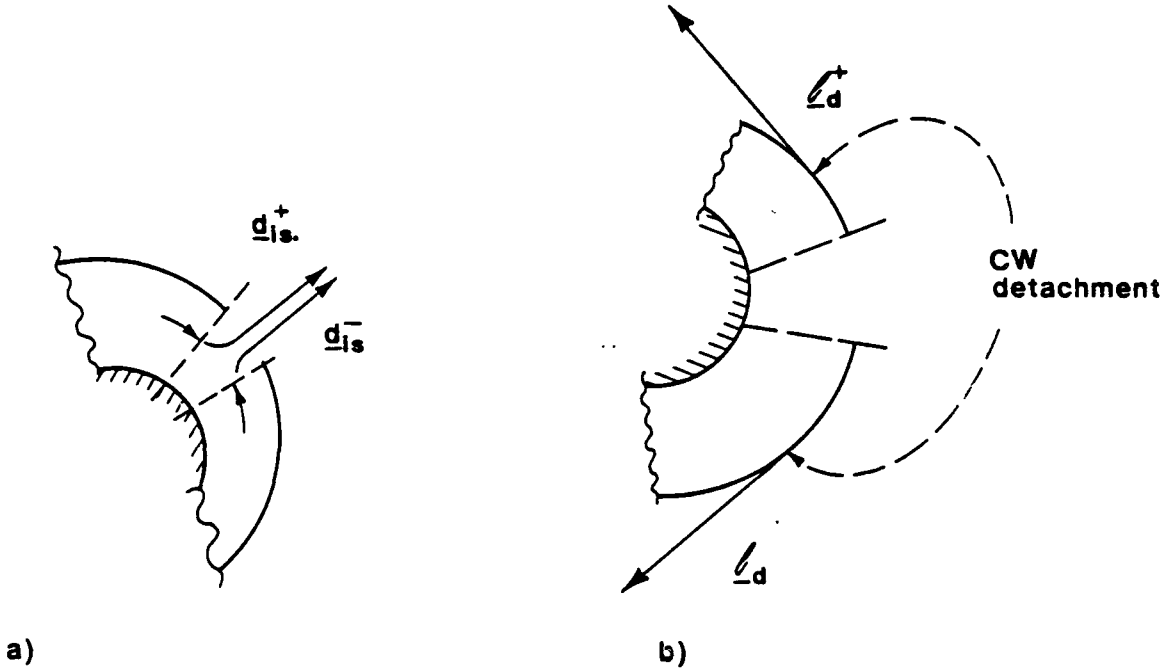


Fig. 3 Ray parametrization of radiation terms: (a) illuminated region, (b) shadow region.

Driving Terms: Again as above, one may identify in \underline{B}_{ag}^{sc} terms due to direct illumination ($\underline{D}_{io}, \underline{D}_{eo}$) or due to CW launch when the slit is on the shadowed region of the shell (\underline{L}_Q) (Fig. 4)

Direct Slit Diffraction: When combining the ray parametrizations of driving (\underline{B}_{ag}) and radiation ($\underline{\Phi}^{eT} \underline{\Pi} [1 - \underline{S}^e \underline{P}^e]^{-1}$) terms, one can extract from the background portion u_b the direct slit diffraction term u_{dd} (Fig. 5).

D. Expansion in Normal and Resonant Modes

The resonant field u_{res} may be expanded through the spectrum of the eigenvalues λ_m of the transition operator $\underline{X} \underline{S}$ in (6) and the corresponding right and left eigenvectors $\underline{\Psi}_m$ and $\underline{\Psi}_m^\dagger$, respectively,

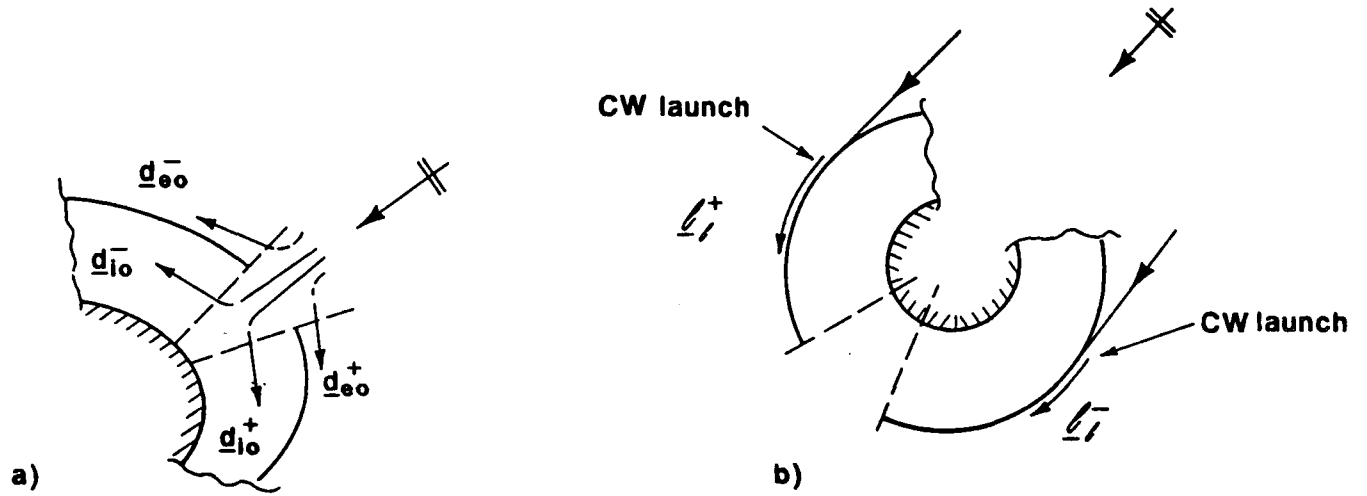


Fig. 4 Ray parametrization of driving terms: (a) illuminated region, (b) shadow region.

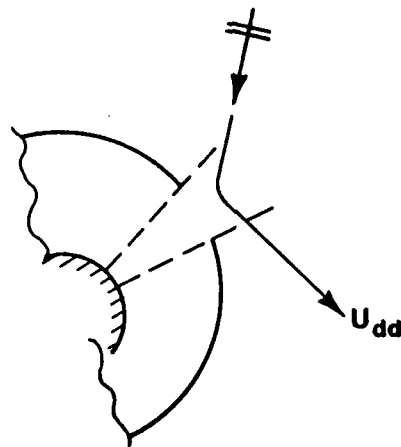


Fig. 5 Direct slit diffraction term (ray parametrization).

$$u_{\text{res}}(\omega) = \sum_m \left(\frac{Q^T(\omega) \Psi_m(\omega) \Psi_m^\dagger(\omega) \underline{I}(\omega)}{1 - \lambda_m(\omega)} \right) u_o \quad (11)$$

The relevant information of u_{res} is contained in its resonances, which can be expressed in the form of a resonant mode (SEM) expansion

$$\sum_{m,n} \left(u_o(\omega) \frac{Q^T(\omega) \Psi_m(\omega) \Psi_m^\dagger(\omega) \underline{I}(\omega)}{-\frac{\partial \lambda_m(\omega)}{\partial \omega}} \right) \bigg|_{\omega=\omega_{mn}} \frac{1}{\omega - \omega_{mn}} \quad (12)$$

with resonance frequencies ω_{mn} specified by

$$\lambda_m(\omega_{mn}) = 1 \quad (13)$$

The resonance excitation coefficients in this expansion are given by projection of the resonant field structure (Ψ_m) onto the incident (\underline{I}) and scattered (\underline{Q}^T) field structure. A detailed manuscript is in preparation [4].

A comprehensive study of the resonance expansions in (11) and (12) is in progress, with emphasis on the effects due to asymmetric interior load conditions.

REFERENCES

- [1] G. Vecchi, "Scattering From a Narrow Axial Slit in a Two-Dimensional Curved Waveguide," in preparation.
- [2] G. Vecchi, in preparation.
- [3] R. Mittra (Ed.), *Numerical and Asymptotic Techniques in Electromagnetics*, Springer Verlag, 1975, Chapt. 6.
- [4] L.B. Felsen and G. Vecchi, "Wave Scattering from Slit Coupled Cylindrical Cavities with Interior Loading: I - Formulation by Ray-Mode Parametrization," in preparation.

B. MICROPARTICLE PHOTONICS

Professor S. Arnold, K.M. Leung and L.M. Folan

Unit EM9-2

1. OBJECTIVE(S)

The main goal of this project is to investigate both experimentally and theoretically the intrinsically nonlinear interaction of intense electromagnetic waves with three-dimensional optically nonlinear structures whose refractive indices are functions of the intensity of the local electric field. These structures can have sizes which are small or large when compared with the wavelength. Our research program will first be directed to the study of isolated structures with well-defined geometries. The results will then be extended to include collections of these microstructures either randomly distributed in a gaseous environment or embedded in regular arrays inside a transparent host medium. Our aim is to understand, on one hand, the limitations on the performance of electromagnetic systems due to scattering and absorption by particles suspended along the propagation path, and on the other, to establish a new approach to nonlinear electromagnetic problems, with a view towards developing a whole new class of optical devices and a new discipline, best called microparticle photonics.

2. SUMMARY OF RECENT PROGRESS

In this section we will review our recent progress since the last report in December 1988. A number of areas of progress associated with Microparticle Photonics will be briefly discussed. In the next section each of these advances will be elaborated on in greater detail.

Our experimental emphasis over the last year has been in attempting to understand the manner in which photon modes within individual particles influence photonic properties. Work on the optical bistability (OB) of an aqueous particle is an example of just such a study. By utilizing a catastrophe based model including all partial waves of the spherical structure we have been able to explain "hidden resonances" which appear in the frequency response and have uncovered odd behavior associated with perturbative coupling between modes of different generic classes. In a second study we have generated a particle $\sim 15\mu$ in diameter with an exceedingly large χ^3 by utilizing an "artificial Kerr Medium" consisting of 50 nm particles in suspension. Here we also observe OB, however the phenomenon is explained heuristically. Finally, since we recognize that nonlinear optical phenomena such as OB have threshold levels which decrease as the photon lifetime increases, we have begun to question the fundamental limits on this time.

On the theoretical side, we have calculated numerically using two independent methods the photonic bands of microparticle superlattice structures. Results are obtained and analyzed for the scalar wave equation. A common gap in the photonic density of state is found to persist down to a relative dielectric constant of about 2.9. A significant variation of the optimal volume filling factor with the relative dielectric constant is found.

3. STATE OF THE ART AND PROGRESS DETAILS

A. Optical Bistability of an Aqueous Microparticle

Near the beginning of this contract we discovered that an isolated spherical liquid microparticle could act as an optically bistable element [1]. Our interpretation of this phenomenon was based on representing the volume averaged intensity within the particle, at a partial wave resonancer, as simple Lorentzian and demanding that the frequency of this resonance change in proportion with this intensity. This model was convenient since the mathematics for treating the problem had already been developed [2]. Unfortunately, such a heuristic model cannot anticipate the mixing of different partial waves due to small distortions of the boundary, or the possibility that standard conventions associated with determining the switching points, from the response function, might not apply. Evidence for the need for a more complete model surfaced with the discovery of so-called "hidden resonances" [3]. These anomalous features occur in regions in which the light scattering associated with different partial wave resonances overlap. In order to provide a more realistic picture of the OB we decided to construct a catastrophe-based graphical model in which all partial wave resonances are taken into account.

The first step in the model was to allow the optical size, X , of the particle to change with both absorption efficiency, Q_a , and intensity, I ,

$$X(X_0, I) = X_0 - \alpha' Q_a(X) I, \quad (1)$$

where X_0 is the optical size at zero intensity and α' is a constant. The nonlinearity in (1) arises from the nature of $Q_a(X)$. For a spherical particle $Q_a(X)$ is composed of Riccati-Bessel functions of complex arguments. No analytical solution to (1) has been found, however, a graphical solution is easily constructed based on representing $Q_a(X)$ from Mie theory. Figure 1 shows the basic scheme for predicting the scattered light response. It starts with Fig. 1a in which the straight line described by $Q_a = (X_0 - X)/\alpha' I$ is plotted along with $Q_a(X)$ as calculated from Mie theory. The points of intersection for a given straight line correspond to the solutions for X . If we suppose for the moment that it is the circumference which changes from one solution to the next, then Q_a may be plotted vs. wavelength (Fig. 1b). Here we clearly see the potential for switching. In the other two frames within Fig. 1 the scattering response is constructed by mapping the solutions from Fig. 1a on the scattering response calculated from Mie theory (Fig. 1c) in order to obtain the level of scattering

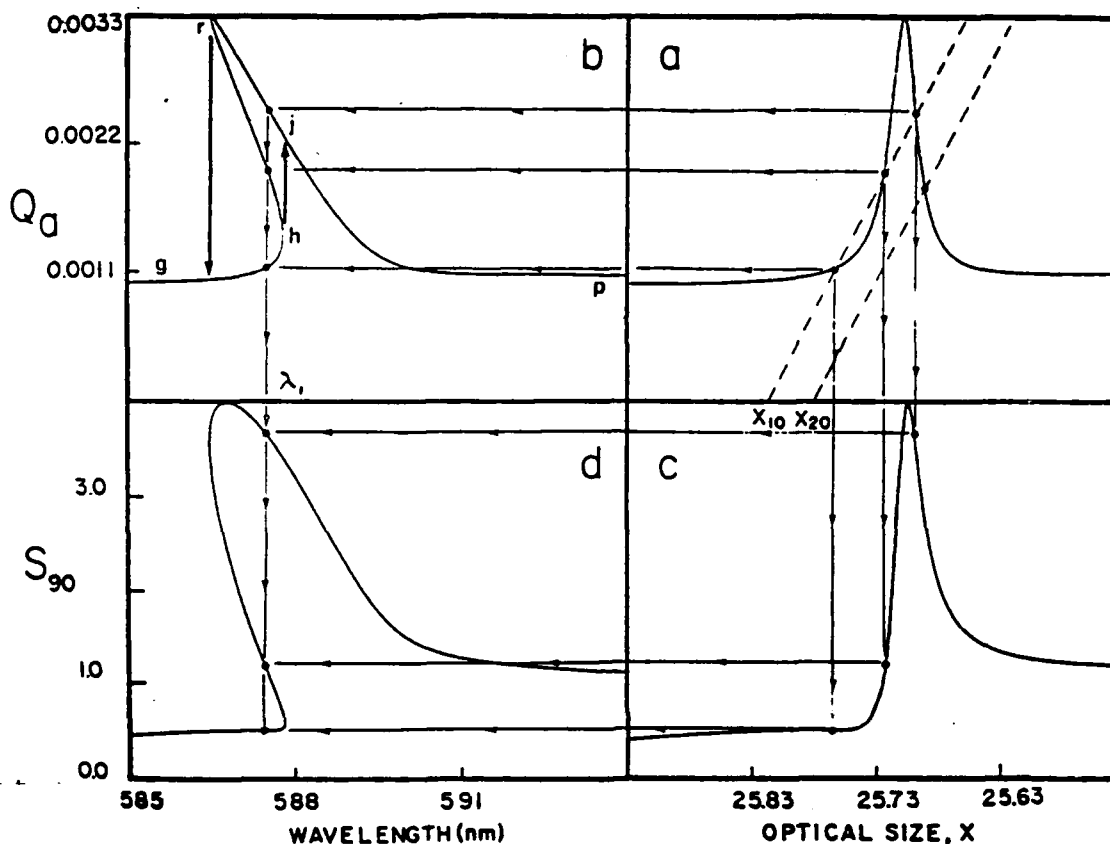


Fig. 1 Catastrophe scheme for single spherical particle

for each solution. These solutions are then displayed vs. wavelength in Fig. 1d.

To test our scheme (Fig. 1) data was taken on a single spherical solution particle [20% $(\text{NH}_4)_2\text{SO}_4$ (by mass) and a crystal violet dye at a concentration of 10^{-5}M], 8.03μ in radius, while levitated in an electrodynamic levitator-trap (Fig. 2b). This frequency spectrum was taken at a scan rate of 0.2 nm/sec. Note that the forward scan shows little resemblance to the reversed scan. In this respect, the γ points in the forward scan provide no visual evidence for the radical departure in the scattering which takes place at these points between the forward and reversed scans. However, a calculation of the response function in this region (Fig. 2a) clearly shows that the γ points are associated with TE modes which are normally hidden in scattering for our experimental observation point. The overall scattering response (analogous to the example in Fig. 1d) is shown in Fig. 2c. As one can see, most aspects of the data are explained by allowing transitions to take place at points in the response function having infinite slope. This strategy corresponds to the "delay convention" in catastrophe theory, a choice usually used for situations for which noise does not

dominate the dynamical process. One notable exception, however, is the hysteretic behavior which begins at the α points in the reverse scan. It should be noted that the width of this hysteretic behavior does not follow the delay convention; the behavior appears to terminate before the point of infinite slope is reached (Fig. 2c). A clue to the origin of this effect is to notice that the actual point of termination is marked by the appearance of other modes. For example the α_3 point which clearly has the $TM_{95,3}$ resonance as the origin for the hysteresis demonstrated in the reversed scan, appears to terminate at a wavelength at which the $TE_{91,4}$ mode can be simultaneously excited (as indicated by the dashed vertical line in Fig. 4). It is interesting to note that this behavior can be described by the Maxwell convention [4]. In contrast to the delay convention the Maxwell convention is expected to be much more appropriate near the α points where dynamical effects associated with a relatively large noise level are important. In particular the noise which is attendant during hysteresis is due to small changes in the shape of the particle from its normal spherical shape. These shape changes disallow a pure spherical modal function, although in many cases one may represent the perturbed wave function for these distorted shapes in terms of a superposition of spherical modes [5]. Thus it is possible for intermode coupling to occur which can lead to switching to a nearby mode [6].

B. Optical Bistability in Other 3-D Systems

The catastrophe model is clearly an effective way of describing the OB of an aqueous microparticle. Bistability in other 3-D systems may be anticipated if an associated value of α' can be estimated. Clearly in the case of a thermal refractive index change in a glass sphere in a time which is considerably longer than the thermal diffusion time, there is no problem. However as soon as one enters the realm in which spatial changes in refractive index induced directly by the light intensity are all there is, the ability to make estimates vanishes due to a lack of analytical theory associated with nonlinear waves in 3-D. So the question is: can one anticipate an OB effect in a spherical structure caused by a local optical nonlinearity (e.g. a Kerr effect)? Pulsed experiments on small microparticles are less convenient and more difficult than CW laser measurements like those shown in Fig. 1. However, this means trying to find a system with an exceedingly large $\chi^{(3)}$ so that the slower thermal effects can be ignored. With luck we have found such a system. This system utilizes small dielectric particles (500 Å diameter) in residence within a Mie size particle which is principally composed of a sugar solution (this host solution keeps the particles from coagulating). The large optical nonlinearity is produced by dielectrophoretic effects within the Mie sized particle [7]. The Maxwell stresses drive the small particles to regions of high intensity. The competition between these Maxwell stresses and thermal fluctuations leads to an overall change in local refractive index which may be modeled as an "artificial Kerr medium" with an exceeding large Kerr coefficient. The preliminary results are encouraging with a clear observation of optical bistability in a situation in which no

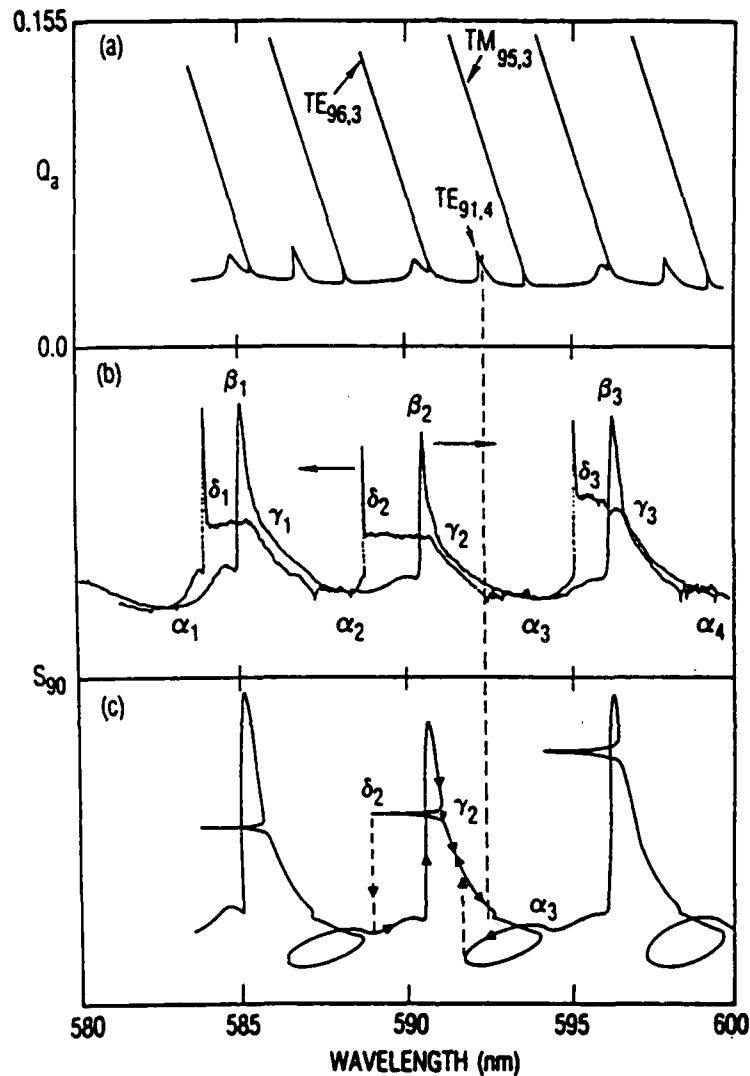


Fig. 2 Comparison of catastrophe model ((a) and (c)) with experimental data (b).

"effective" mass change is produced (i.e. no apparent size change occurs). These experiments provide the first data on an "artificial Kerr medium" from which we should be able to extract α' . Thus a heuristic model has the potential of being built.

While the aforementioned work is in motion, we are beginning to form glass particles with traditional to large $\chi^{(3)}$ values. Here the interest is "real world" photonic elements which can have potentially fast switching speeds, and perhaps more important, can be approached with lasers from any direction. In addition to this obvious difference with traditional photonic elements (e.g.

Fabry-Perot resonators), the dielectric confinement associated with high symmetry 3-D objects such as spheres allows the possibility of low intensity switching. Recently, three groups [8-10] have shown that Q values associated with the resonances of a liquid microsphere can approach 10^7 . This value has been shown theoretically to be limited only by stochastic thermal fluctuations at the surface [11]. Since elastic constants of glass particles are orders of magnitude larger than those of typical liquids one can conceive of Q values approaching 10^{10} .

C. Photonic Band Structures in Microparticle Superlattices

During the last year, our theoretical interest has focused on the interaction of electromagnetic waves in three-dimensional periodic dielectric structures. Such structures can be fabricated, for example, by embedding microparticles regularly within a host medium. By analogy to electron waves in a crystal, the idea of photonic band structure must be introduced, together with the concepts of reciprocal space, Brillouin zones, van Hove singularities, etc. [12,13].

If the depth of dielectric constant modulation is sufficiently large, then a photonic band gap will open up in the photonic density of states. Within this band gap, optical modes and spontaneous emission are all absent. The possible applications of such a gap are rather interesting. First, spontaneous emission at frequencies within this gap will be strongly inhibited [12]. A similar effect has in fact been demonstrated, albeit only under some rather extreme experimental conditions [14,15]. The ability to inhibit spontaneous emission has some extremely important consequences since spontaneous emission plays a fundamental role in limiting the performance of semiconductor lasers, heterojunction bipolar transistors, and solar cells [12,16]. Second, it has been suggested that atomic and molecular physics is profoundly modified in a volume of space in which the most important electromagnetic processes are totally suppressed [17]. In particular, the resonant interaction, potential of homonuclear diatomic molecules, as well as many other atomic physical properties are severely modified in such a spatial region. Third, there have also been proposals to study mobility edges and Anderson localization of photons within such a forbidden gap by introducing some randomness into the structure [12,17].

From rather basic considerations, it is clear that there are criteria that must be met in order to create such band gaps. The electromagnetic waves must scatter sufficiently strongly with the superlattice structure so that band gaps are large enough to have a common overlapping frequency region. This means that the dielectric modulation must be fairly high, and the microparticle size and particle-particle distance must be comparable to the wavelength of light where the gap is intended to be located. Moreover, the scattering must have almost equal strength for all wavevectors lying at the boundary of the first Brillouin zone so that the gaps will have the largest overlap. This means that the Brillouin zone should be as spherical as possible.

To see if a common gap can in fact exist in superlattice structures which can be fabricated with materials currently available in the optical range, an experiment at microwave frequencies was performed by Yablonovitch at Bellcore [19]. Out of 21 samples prepared, only one showed a common gap. This Edisonian approach is extremely time consuming. Our goal here is to apply a variety of theoretical methods, including exact numerical calculations of photonic band structures and analytical studies to help interpret the experimental data, and to make calculations that will help determine the optimal configuration for creating such a gap.

At present, the only reported calculation was done by the Princeton group for a face-centered cubic lattice of microparticles [18]. The Korringa-Kohn-Rostoker (KKR) method [20,21] was used with the scalar wave equation, ignoring the vector nature of light. There are two major findings in this work: (i) The optimal volume filling fraction of microparticles for the creation of a common gap is approximately 10%. (ii) The gap persists for relative dielectric constant, r , as small as 7.8.

We have repeated their calculations using the same KKR method. Results for the photonic band structure for $r=12.25$ and a volume filling factor $f=0.375$ are shown in Fig. 3 as open circles. Although qualitatively our results agree with those of the Princeton group, quantitatively there are significant differences in a few of the important findings. We find that the gap actually persists until r is about 2.9, as compared with 7.8 in the Princeton study. Moreover, we find that the optimal volume filling factor, f , has a significant dependency on r , as shown in Fig. 4. This dependency is exactly what should be expected on physical grounds. At each given value of r , the maximum band gap at the optimal volume filling factor is also found. The result is shown in Fig. 5. We believe that our numerical results are in fact correct. We have performed two important checks on our results: (i) We made an analytical study of the dispersion relation in the low-frequency limit and found that our numerical results agree to within our computational accuracy, which is about 0.1%. (ii) We repeated our band structure calculations using the plane-wave method. Amazingly, the method converges very fast. The results are shown by the solid circles in Fig. 3, and can be seen to be almost indistinguishable with our KKR results.

As present, we are in the process of calculating the band structure for the full Maxwell's equations. We are very optimistic that our findings will explain the experimental data, and will help to find the most optimal configuration for the creation of photonic gaps in this new class of artificial optical media.

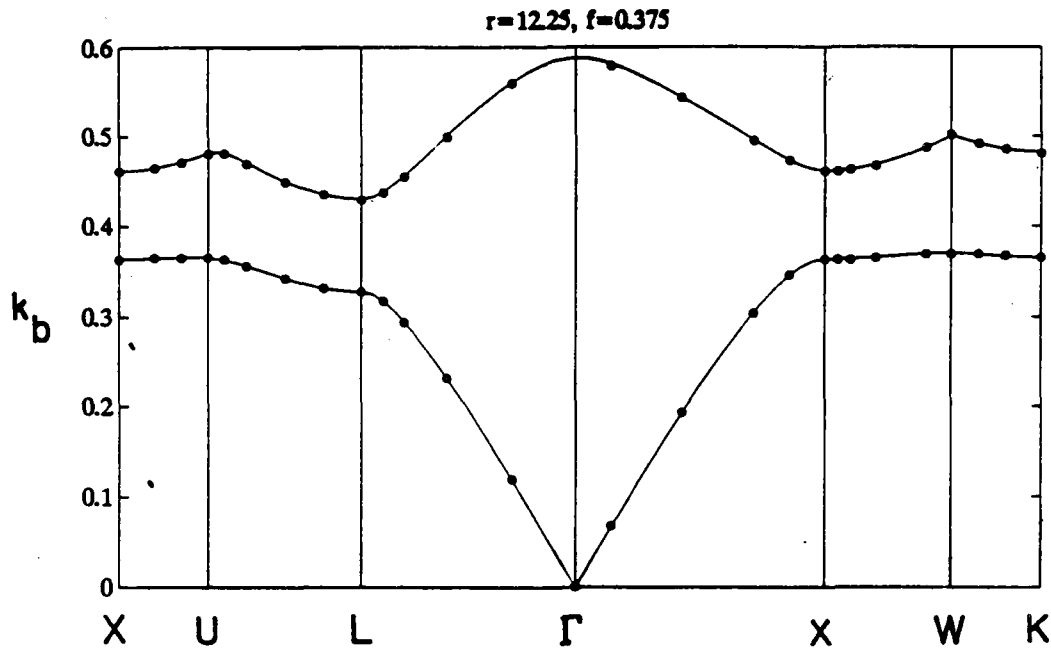


Fig. 3 The solid curves give the band structure calculated with the plane wave method. The volume filling fraction of spheres is 0.375 and the relative dielectric constant is 12.25. The closed circles are our results calculated with the KKR method.

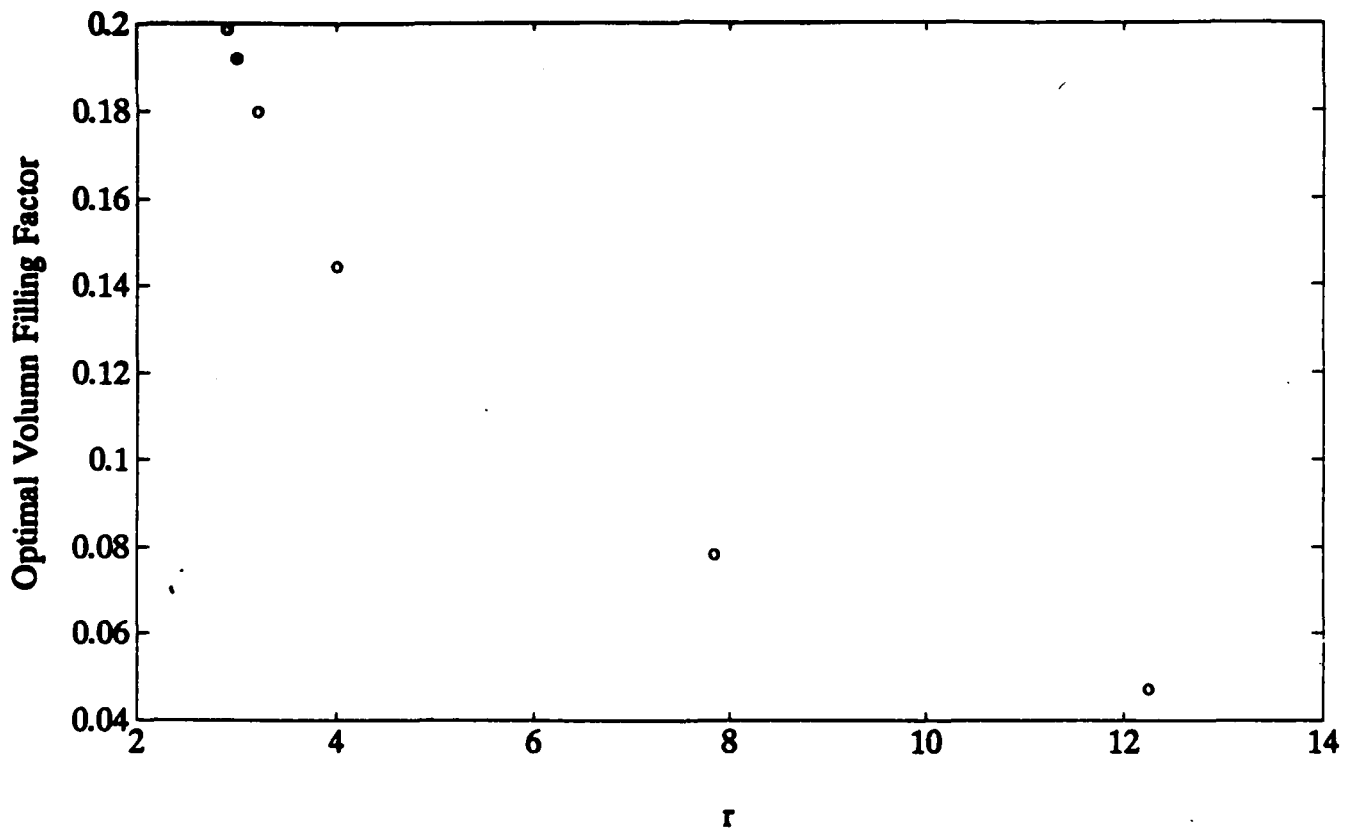


Fig. 4 The optimal volume filling fraction of spheres for the creation of a gap in the photon density of states is plotted as a function of the relative dielectric constant.

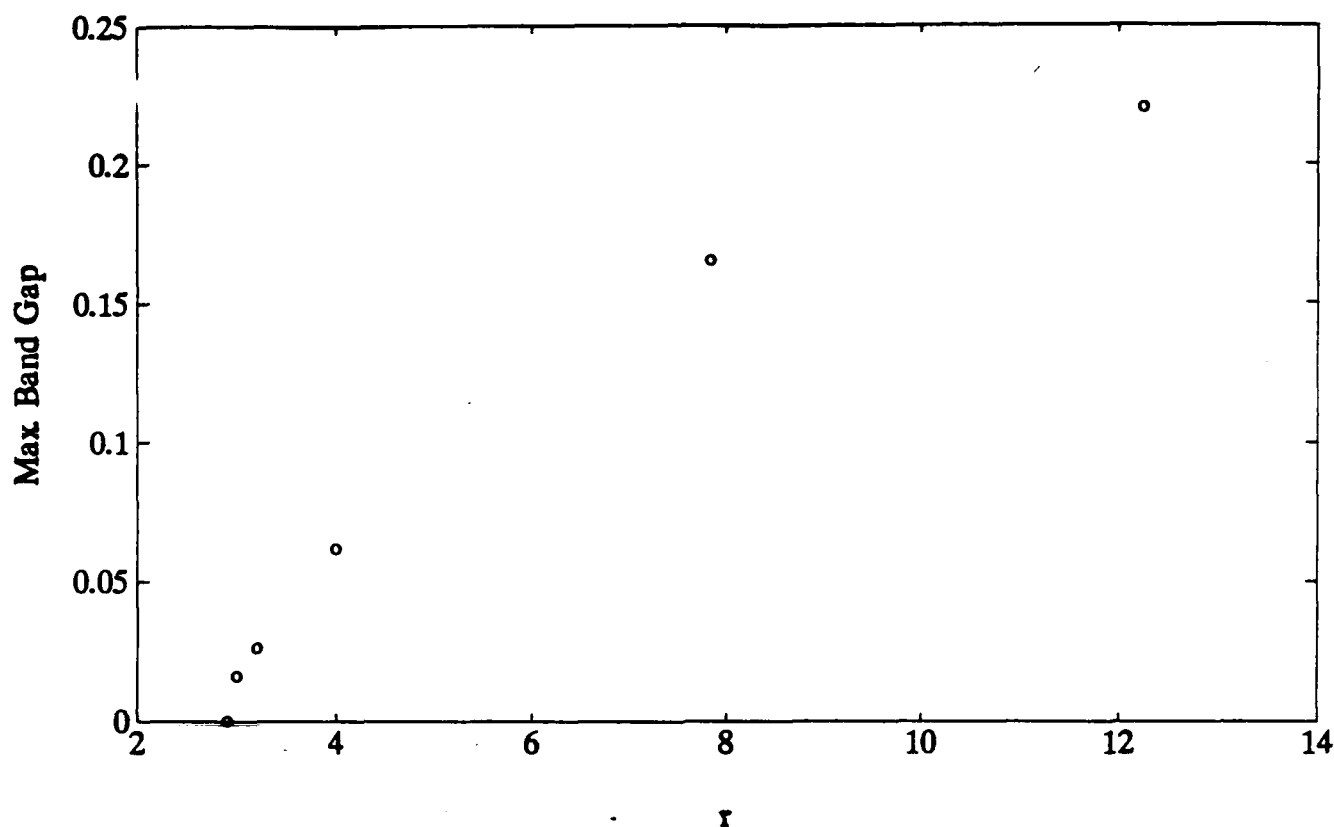


Fig. 5 The size of the gap at the optimal volume filling fraction is shown as a function of the relative dielectric constant.

4. REFERENCES

1. S. Arnold, M. Leung and A.B. Pluchino, *Opt. Lett.* **11**, 800 (1986).
2. K.M. Leung, *Phys. Rev. A* **33**, 2461 (1986).
3. S. Arnold, L.M. Folan and T. Scalese, *Bull. Am. Phys. Soc.* **32**, 566 (1987).
4. R. Gilmore, *Catastrophe Theory for Scientists and Engineers*, (J. Wiley, New York, 1981), Ch. 8, p. 141-156.
5. H.M. Lai, P.T. Leung and K. Young, "Time-independent Perturbations for Leaking Electromagnetic Modes in Open Systems with Application to Resonances in Micro-droplets," *Phys. Rev. A* (in press).
6. S. Arnold, T.R. O'Keeffe, K.M. Leung, L.M. Folan and T. Scaleseed (in preparation).
7. P.W. Smith, P.J. Maloney and A. Ashkin, *Opt. Lett.* **7**, 347 (1982).
8. S. Arnold and L.M. Folan, *Opt. Lett.* **14** 387 (1989).
9. J.-Z. Zhang, D.H. Leach and R.K. Chang, *Opt. Lett.* **13**, 270 (1988).

10. R.G. Pinnick et al., Opt. Lett. **13**, 494 (1988).
11. H.M. Lai, P.T. Leung and K. Young, Phys. Rev. A (in press).
12. E. Yablonovitch, Phys. Rev. Lett. **58**, 2059 (1987).
13. S. John, Phys. Rev. Lett. **58**, 2486 (1987).
14. K.H. Drexhage, in *Progress in Optics*, edited by E. Wolfe (North-Holland, Amsterdam, 1974), Vol. 12, p. 165; R.R. Chance, A. Prock and R. Silbey, in *Advances in Chemical Physics*, edited by I. Prigogine and S.A. Rice (Wiley, New York, 1978), Vol. 37, p. 1.
15. R.G. Hulet, E.S. Hilfer and D. Kleppner, Phys. Rev. Lett. **55**, 2137 (1985).
16. E. Yablonovitch, T.J. Gmitter and Bhat, Phys. Rev. Lett. **61**, 2546 (1988).
17. G. Kurizki and A.Z. Genack, Phys. Rev. Lett. **61**, 2269 (1988).
18. S. John and R. Rangarajan, Phys. Rev. B **38**, 10101 (1988).
19. E. Yablonovitch and T.J. Gmitter, Phys. Rev. Lett. **63**, 1950 (1989).
20. J. Korringa, Physica **13**, 392 (1947).
21. W. Kohn and N. Rostoker, Phys. Rev. **94**, 1111 (1954).

C. BEAM-FIELD INTERACTION WITH NONLINEAR THIN FILMS

Professors K. Ming Leung and Theodor Tamir

Unit EM9-3

1. OBJECTIVE(S)

The aim of this project is to investigate a new class of electromagnetic phenomena that involve bounded beams propagating under nonspecular regimes in the presence of planar nonlinear media. These phenomena are produced by the combination of (a) unexpectedly large nonspecular effects involving beams in thin films, with (b) the field-modification behavior of dielectric layers whose refractivity is intensity-dependent. The overall effects include beam displacements of the lateral, angular and longitudinal types, field focusing or fragmentation, as well as other varieties of field changes and beam distortions.

By exploiting the action of nonlinearities to enhance and modify the nonspecular effects, novel techniques for dynamically controlling beam trajectories can be explored. These techniques will thus be useful in the design of optical components and in the implementation of optoelectronic devices.

2. SUMMARY OF RECENT PROGRESS

During the past period, our investigation has considered two major aspects involving propagation of fields in or along nonlinear layers. First, we have obtained exact analytical results for the interaction of plane TM polarized wave with a nonlinear dielectric thin film. Our results apply to both scattering and guided wave cases, and to any nonlinear film whose dielectric constant is a function of intensity. In addition, we have developed a highly accurate "cubic approximation", which is valid under most experimental conditions. This approximation, although is in principle unnecessary, enables all the results to be obtained explicitly and analytically in terms of known functions, and thus facilitates a detailed investigation of all possible effects within the entire physical parameter region.

In a parallel second study, we have investigated the field behavior at the boundary to a nonlinear medium when a beam field is incident upon it. Our previous analytical study of a specific beam-like field, namely the nonlinear leaky wave reported previously, was viewed in the context of beams that propagate without decay. In particular, we have explored the incident beam profile required to generate a single soliton in the nonlinear medium. The mathematical approach has produced ample information about the interaction of beam fields at a nonlinear interface. In turn, this information will be applied to analyze a broad class of field varieties which are important in the design of

nonlinear optical devices.

3. STATE OF THE ART AND PROGRESS DETAILS

Recent work on the interaction of electromagnetic waves with nonlinear dielectric films having intensity-dependent refractive indices has revealed [1,2] a number of remarkable phenomena which have stimulated the development of many ultra-fast and compact all-optical and optoelectronic devices. Besides their compactness, nonlinear thin-film devices have the additional advantage that the waves inside the film can be compressed to a dimension comparable to a wavelength, or even smaller, so that nonlinear processes which depend sensitively on the field intensity can be drastically enhanced [3]. Moreover, the waves can be guided along the film through a great distance, thereby providing a long path for the interaction and mixing of the waves and thus further enhancing the nonlinear effects. However, most theoretical results reported so far in this area have assumed that the incident field is a plane wave. This is often an inadequate assumption even in the low intensity (linear) limit. In fact, by considering incident bounded beams instead of plane waves, lateral beam displacements have been identified [4-11] even in linear dielectric or metallic layers. Most recently, we have reported [12] an entire set of fascinating nonspecular effects which include not only large lateral beam displacements, but also focal and angular beam shifts, anomalous absorption phenomena and strong beam-profile deformations. Analogous effects occur for transmitted (refracted) beams [9].

In the nonlinear regime, on the other hand, a beam wave can undergo self-focusing or self-fragmentation even in an infinite homogeneous medium [13]. In a one-dimension spatially homogeneous medium, detailed studies have conclusively indicated [14] that the propagation characteristics of nonlinear waves depend crucially on the initial wave profile. Furthermore, a huge lateral beam shift of the Goos Hanchen type has already been reported [15]. All these considerations indicate that the presence of nonlinear thin films can drastically modify the plane-wave results and significantly magnify nonspecular effects which are large already in the absence of nonlinearities.

Work in this area has also emphasized [2] effects associated with optical-bistability phenomena which, of course, have tremendous potentials for a variety of device applications. However, bistability is associated with an intrinsic nonlinear behavior that has no counterpart in the linear regime and cannot, in fact, exist unless the incident power is above a threshold level [16,17]. By contrast, the phenomena considered here involve nonlinearities which account for fields that are not subject to threshold effects but, in the limit of very weak intensities, their behavior reduces to that of linear media. The nonlinear situations to be studied are therefore inherently different from those leading to bistability and, in particular, they can be regarded as generalized analogs of the particular linear case.

The nonlinear generalized analogs addressed by our research program consist of planar configurations that contain one or more layers whose refractivity is field-intensity dependent. A principal concept motivating this research is that, by judiciously combining the effects of nonlinearities with the nonspecular behavior of beam fields, new beam-controlling techniques can be developed for application to thin-film optical components. In this context, our studies during the past period have dealt with the two inter-related aspects outlined below.

A. Interaction of Plane TM Wave with Nonlinear Film

Thus far, the majority of work on the interaction of plane electromagnetic waves with nonlinear dielectric thin film has focussed on TE polarized waves. This is because the intensity, which changes the dielectric constant within the film, depends only on a single component of the electric field for TE waves. In contrast, for the case of TM polarized waves, the intensity either depends on two separate components of the electric field, or alternately depends on the magnetic field and its derivative in quite a complicated way. For the latter choice for example, the mathematical problem is to solve the magnetic field, B , which can be shown to obey the following second order nonlinear differential equation:

$$\frac{d}{dz} \left[\frac{1}{\epsilon} \frac{dB}{dz} \right] = \left(\frac{k_x^2}{\epsilon} - \frac{\mu \omega^2}{c^2} \right) B, \quad (1)$$

where the dielectric constant depends on B in the following complicated way:

$$\epsilon = \epsilon \left(\left| \frac{1}{\epsilon} \frac{dB}{dz} \right|^2 + \left| \frac{k_x B}{\epsilon} \right|^2 \right). \quad (2)$$

In addition, it should be noted that the argument of ϵ involves ϵ itself also. Because of the difficulty associated with the mathematical problem, theoretical studies on TM waves have been exclusively purely numerical in nature [18,19], so that results have only been obtained for a few specific parameter values, and detailed investigations covering all the possible behaviors have not been made.

The mathematical problem posted above for the TM case has recently been solved exactly and analytically, by finding exact integrating factors for the nonlinear Maxwell's equations, and by appropriately changing the independent variable at a certain stage of the derivation. This work is based on our previous work on the propagation of TM polarized surface guided waves in a semi-infinite nonlinear dielectric medium [20]. The added complication here is due to the fact that B is intrinsically complex, and it satisfies a different set of boundary conditions. We have shown that the solution for the magnetic field can be expressed in terms of quadratures, and our results apply irrespective of the detailed form of the dependence of ϵ on the intensity. The actual derivation is too lengthy to be included here and we will only report some of

the main results.

Our result for the magnetic field is written in terms of an amplitude function, $A(z)$ and a phase function, $\theta(z)$ as follows:

$$B(z) = A \exp(i\theta). \quad (3)$$

We found a first integral for A in the form

$$A^2 = [\epsilon^2 I(\epsilon - \epsilon_0) - \epsilon \int_0^{\epsilon - \epsilon_0} du I(u) + c_2 \epsilon] / (2k_x^2 - \epsilon), \quad (4)$$

where c_2 is an integration constant, $I(\epsilon - \epsilon_0)$ is the inverse function of $\epsilon_2(I)$, and ϵ_0 and $\epsilon_2(I)$ are respectively the linear and nonlinear part of the dielectric constant defined by

$$\epsilon = \epsilon_0 + \epsilon_2(I). \quad (5)$$

By changing the dependent variable from A to ϵ , the second integral can be expressed as

$$z = \int_{\epsilon(0)}^{\epsilon} \frac{d\epsilon}{[-2V(\epsilon)]}, \quad (6)$$

where the "potential function" V is given by

$$V = -\frac{1}{2} \left[\frac{dA(\epsilon)}{d\epsilon} \right] \left[\epsilon^2 I(\epsilon - \epsilon(0)) - k_x^2 A^2(\epsilon) - \frac{c_1^2 \epsilon^2}{A^2(\epsilon)} \right] \quad (7)$$

and $\epsilon(0)$ is the value of the dielectric constant at $z = 0$. Equation (7) gives z as a function of ϵ , and by inverting it we obtain $\epsilon(z)$. Inserting $\epsilon(z)$ into the first integral then gives $A(z)$. The phase function can be obtained by another quadrature:

$$\theta(z) = c_1 \int_0^z dz \frac{\epsilon}{A^2} + \theta_0, \quad (8)$$

where θ_0 is yet another integration constant.

In addition to the above analytical results, we have also shown that, under most experimental conditions, the nonlinearity can be considered weak, and consequently the "potential function" V can be accurately be approximated by a third order polynomial. This procedure then enable us to write explicit analytical solution for the magnetic field, thus allowing us to explore in detail the behavior of the solution over a much larger parameter region.

Although the above results are given specifically for the case of scattering of plane TM waves, by simply setting the integration constant c_1 to zero the results apply equally well to the propagation of TM guided waves in a nonlinear

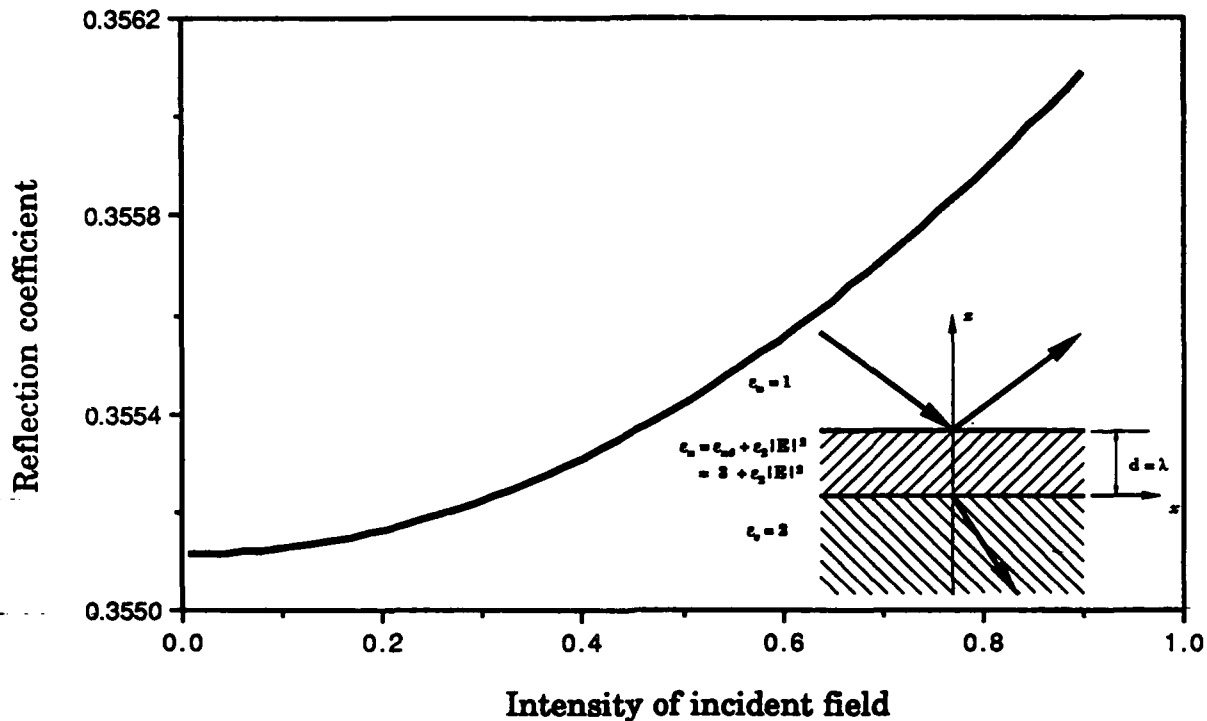


Fig. 1 Reflection coefficient vs. intensity of incident field

dielectric film having an intensity dependent refractivity.

B. Soliton Excitation by a Beam Field Incident onto the Boundary to a Nonlinear Medium

Over the past decade, studies of optical beams in the presence of nonlinear media with intensity dependent refractive indices have demonstrated several interesting and useful phenomena which have helped develop all-optical and optoelectronic devices. In particular, the soliton solution [21] of the nonlinear Schrodinger equation has revealed novel effects it electromagnetic waves interact with nonlinear media [13,22]. In the earlier years, most theoretical results reported in this area assumed that the incident field is a plane wave of infinite extent rather than a realistically bounded beam. This assumption is often a serious limitation when considering nonlinear effects in optical devices. By regarding incident bounded beams instead of plane waves, certain well identified effects in linear regimes, such as lateral beam displacements [4,16] and the coupling of optical beams into guiding structures [7,23], have been explored in the context of nonlinear media.

During the preceding reporting period, we have developed a new approach to leaky-wave fields propagating along a nonlinear waveguide and applied the results to study the operation of nonlinear output prism couplers [24]. However, the study of input couplers requires a more detailed examination of the field behavior when a beam is incident rather than outgoing. We have therefore examined the beam profile required for generating a single TE-type

soliton in a nonlinear medium. For this purpose, we have assumed the geometry shown in Fig. 2 where a soliton is generated in a nonlinear medium with positive Kerr nonlinearity $\epsilon_n = \epsilon_{n0} + \epsilon_2 |E|^2$ located at $z > 0$.

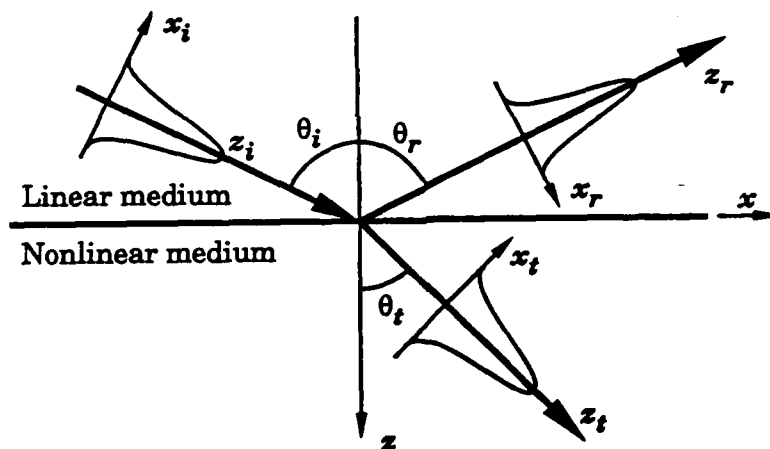


Fig. 2 Illustration of interaction of optical beam with nonlinear interface and soliton emission.

The field of that TE soliton is given by

$$E_y = \left[\frac{2}{\epsilon_2 k_0^2} \right]^{1/2} 2\eta \operatorname{sech}(2\eta x_t) \exp(i\beta z_t). \quad (9)$$

We assume that this soliton emerges at the nonlinear interface after the incident beam interacts with that interface. Invoking the appropriate boundary conditions, we know that the tangential field components are the same on the linear and nonlinear sides of the interface. After properly transforming the (x_t, z_t) coordinates in Eq. (9) into the (x, z) coordinates tied to the boundary, we can assume that the field along that boundary is given by Eq. (9). In principle, we can then derive the field distribution of both incident and reflected beams at any point. To simplify the derivation, we apply a Fourier transform to that boundary field and obtain that the spatial spectrum of the incident field has the following form:

$$e_i(\alpha) = \frac{\pi}{8\eta \cos\theta_t} \left[1 + \frac{\beta(1+\sin^2\theta_t)}{\cos\theta_t \sqrt{k_0^2 - \alpha^2}} - \frac{2\alpha \tan\theta_t}{\sqrt{k_0^2 - \alpha^2}} \right] \operatorname{sech} \left(\frac{\beta \sin\theta_t - \alpha}{4\eta \cos\theta_t} \pi \right) \quad (10)$$

so that the incident beam field is given by the integral

$$E_{yi} = \frac{1}{2\pi} \int_{-\infty}^{\infty} e_i(\alpha) \exp[i(\sqrt{k_0^2 - \alpha^2} x + \alpha z)] d\alpha. \quad (11)$$

Depending on the parameters involved, we have used several methods to evaluate the above integral. For a relatively weak soliton, we expand the integrand and express it in a Gaussian form which can be evaluated easily. In the case of a strong soliton, we apply the steepest-descent method which yields a relatively complicated result, but this still shows a beam-like field.

The result of the Gaussian approximation is illustrated in Fig. 3, which depicts a beam incident from a linear region onto an interface to a nonlinear medium. Part of the incident power is reflected back, but the remainder is transmitted and generates a soliton in the nonlinear medium. For strong soliton cases, the profile of the incident beam in Fig. 3 may be asymmetric and different from Gaussian.

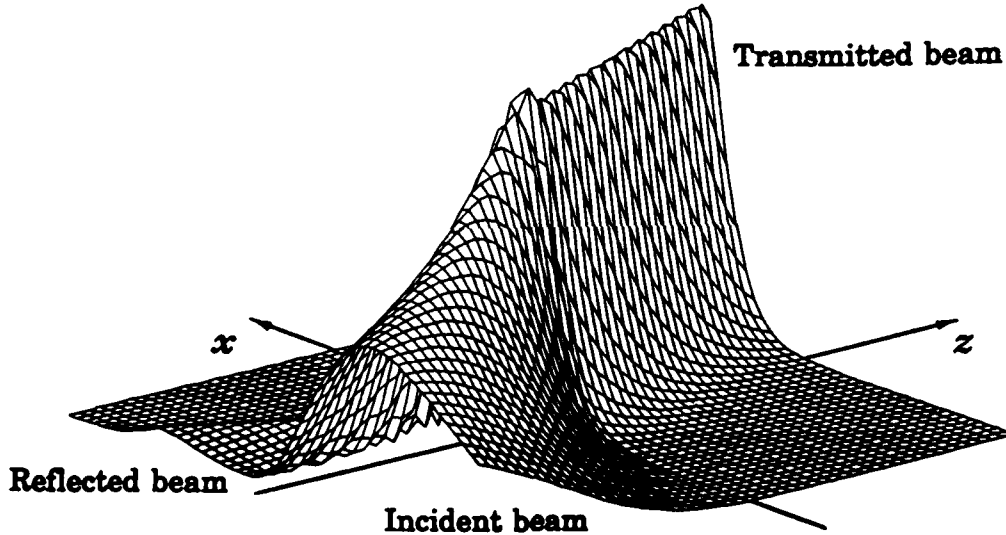


Fig. 3 Field profile of incident, reflected beam and transmitted soliton.

Based on these first results of beam-field solutions, we plan to continue our investigation of such situations involving nonlinear media in the presence of realistic boundaries and well confined beam fields. As already worked out during the preceding year, we then plan to apply such results to nonlinear optical devices, such as beam couplers, switches and other applications.

4. REFERENCES

- [1] G.I. Stegeman and C.T. Seaton, "Nonlinear surface polaritons", in *Dynamical Phenomena at Surfaces, Interfaces, and Superlattices*, ed. by F. Nizzoli, K. H. Rieder and R.F. Willis (Springer Series in Surface Sciences, Springer-Verlag, NY, 1985).
- [2] H. M. Gibbs, P. Mandel, N. Peyghambarian, and S.D. Smith, *Optical Bistability III* (Springer-Verlag, NY, 1986).
- [3] G.I. Stegeman, "Guided wave approach to optical bistability", *IEEE J. Quant. Electron.* QE-18, pp. 1610- 1619; October 1982.
- [4] T. Tamir and H.L. Bertoni, "Lateral displacement of optical beams at multilayered and periodic structures", *J. Opt. Soc. Amer.* 61, pp. 1397-1413; October 1971.
- [5] W.P. Chen and E. Burstein, "Narrow beam excitation of electromagnetic modes in prism configurations", in *Electromagnetic Surface Modes*, A.D. Boardman, ed. (Wiley, London 1982), pp. 549-574.
- [6] V. Shah and T. Tamir, "Absorption and lateral shift of beams incident upon lossy multilayered media", *J. Opt. Soc. Amer.* 73, pp. 37-44; January 1983.
- [7] C.W. Hsue and T. Tamir, "Lateral beam displacements in transmitting layered structures", *Optics Commun.* 49, pp. 383-387; April 1984.
- [8] P. Mazur and B. Djafari-Rouhani, "Effect of surface polaritons on the lateral displacement of a light beam at a dielectric interface", *Phys. Rev. B* 30, pp. 6759- 6762; December 1984.
- [9] C.W. Hsue and T. Tamir, "Lateral displacements and distortion of beams incident upon a transmitting-layer configuration", *J. Opt. Soc. Amer. A*, 2, pp. 978-988; June 1985.
- [10] R.P. Riesz and R. Simon, "Reflection of a Gaussian beam from a dielectric slab", *J. Opt. Soc. Am. A*, 2, pp. 1809-1817; December 1985.
- [11] S.L. Chuang, "Lateral shift of an optical beam due to leaky surface-plasmon excitations", *J. Opt. Soc. Am. A*, 3, pp. 593-599; May 1986.
- [12] T. Tamir, "Non-specular phenomena in beam fields reflected by multilayered media" *J. Opt. Soc. Amer. A*, 3, pp. 558-565; April 1986.
- [13] S.A. Akhmanov, A.P. Sukhorukov and R.V. Khokhlov, *Sov. Phys. Uspekhi*, "Self-focusing and diffraction of light in a nonlinear medium", *Sov. Phys. Uspekhi*, 93, pp. 609-636; March-April 1968.
- [14] M.J. Ablowitz and H. Segur, *Solitons and the Inverse Scattering Transform* (SIAM, Philadelphia, 1981).

- [15] W.J. Tomlinson, J.P. Gordon, P.W. Smith, and A.E. Kaplan, "Reflection of a Gaussian beam at a nonlinear interface", *Appl. Opt.*, 21, pp. 2041-2051; June 1982. K.M. Leung, "Propagation of nonlinear surface polaritons", *Phys. Rev. A*, 31, pp. 1189-1192; February 1985.
- [16] K.M. Leung, "Optical bistability in the scattering and absorption of light from microscopic particles", *Phys. Rev. A*, 33, pp. 2461-2464; April 1986.
- [17] S. Arnold, K.M. Leung and A.B. Pluchino, "Optical bistability of an aerosol particle", *Opt. Lett.* 11, pp. 800-802; December 1986.
- [18] A.D. Boardman, A.A. Maradudin, G.I. Stegeman, T. Twardowski and E.M. Wright, "Exact theory of nonlinear p-polarized optical waves", *Phys. Rev. A*, 35, pp. 1159-1164; February 1987.
- [19] A.D. Boardman and T. Twardowski, "Transverse-electric and transverse-magnetic waves in nonlinear isotropic waveguides", *Phys. Rev. A*, 39, pp. 2481-2492; March 1989.
- [20] K.M. Leung, "p-polarized nonlinear surface polaritons in materials with intensity-dependent dielectric functions", *Phys. Rev. B*, 32, pp. 5093-5101; October 1985.
- [21] V.E. Zakharov and A.B. Shabat, "Exact theory of two-dimensional self-focusing and one-dimensional self-modulation of wave in nonlinear media", *Sov. Phys. JETP* 34(1), pp. 62-69; January 1972.
- [22] A.B. Aceves, J.V. Moloney and A.C. Newell, "Theory of light-beam propagation at nonlinear interfaces: I. Equivalent-particle theory for a single interface", *Phys. Rev. A* 39, pp. 1809-1822; February 1989.
- [23] R. Ulrich, "Theory of the prism-film coupler by plane-wave analysis", *J. Opt. Soc. Amer.* 60, pp. 1337-1350; October 1970.
- [24] L. Lin, T. Tamir and K.M. Leung, "Leaky-wave modes in nonlinear output prism couplers", *Appl. Phys. Lett.* 55 (5), pp. 427-429; July 1989.

D. HYBRID METHODS FOR WAVE PROPAGATION AND SCATTERING

Prof. I-T. Lu

Unit EM9-4

1. OBJECTIVE(S)

This project is to address a use of the combination of local scattering operators (moment method, boundary-finite elements, etc.) and the global operators (ray-mode, image-mode, etc.) to study wave coupling through apertures or wave scattering phenomena by obstacles in a layered media. During last year's investigation, several problems with similar geometric structure, but governed by different system equations, were identified and detailed investigations have been performed. One important area is analysis of various microwave devices (such as transmission lines, filter, couplers, etc.). Both quasi-TEM approximation and full wave analysis are considered. Wave scattering from aperture coupled systems is also studied, which is relevant to technologies concerning electromagnetic radiation, leakage, compatibility, interference, and shielding. Another area is analysis for acoustic emission or scattering by obstacles in shallow water or open environment. This study is relevant to both passive and active sonar applications for detecting and localizing a target.

2. STATE OF THE ART

For wave propagation and scattering in complicated environments, no one single solution method can work satisfactorily for a broad range of parameters. Spectral methods, such as spectral integration, mode expansion, and generalized ray expansion, only work for separable geometries. Low frequency methods, such as method of moments, T-matrix, finite elements, boundary elements, and finite difference, are convenient for small size structures, but are too computer intensive for large media. High frequency methods, such as asymptotic ray theory and Gaussian beam method, are flexible enough to be adapted to non-planar and inhomogeneous layered media, but fail when media properties vary rapidly. Therefore, it may be advantageous to combine various analytic, asymptotic, or numerical algorithms into a single framework to optimize the advantages of each.

In the wave equation, we have three configurational and one temporal coordinates. The most general hybrid method can be constructed by partitioning the four-dimensional space into subregions. In every subregion the temporal coordinate defines a time spectrum, and each configurational coordinate defines a local spectral domain. The solution in the subregion can then be solved in the original coordinate system, transformed domain, or mixed (phase) domain. Furthermore, there are various ways of partitioning

spectra and of performing inverse transform(s). Therefore, there are usually many solution methods available for each subregion, and proper options must be chosen to provide physical insights and to ensure numerical efficiency and accuracy (hybrid methods may be desired even in some subregions). To integrate various methods in these subregions, we impose boundary conditions at the interfaces between subregions. The field variables along these interfaces are then formulated in terms of system equations which are to be solved numerically. Efficient iterative schemes for solving the system equations are available when the coupling among subsystems is weak.

In the last year, we consider multiple inhomogeneous scatters embedded in a waveguide. We also consider multiple apertures on the walls of a waveguide. Typical global propagators of the waveguide, local scattering operators of the scatters or apertures, and a systematic way of combining them are discussed as follows.

A. Global Propagator

For propagation in a stratified medium, discrete or continuous transforms can be applied to one or two of the lateral coordinate(s). The remaining two or one transverse coordinate(s) can then be solved by numerical methods (such as finite elements and finite difference), analytic methods (such as characteristic Green's functions, invariant embedding, reflectivity, propagator, etc.), or asymptotic methods (such as WKB). Therefore, many alternative numerical schemes are available. According to the ways of partitioning spectra and of performing inverse transform(s), we have spectral integrals, modes, generalized rays, ray-mode, etc. If the medium properties are not laterally invariant, the exact transform theory fails. Nevertheless, local modes, asymptotic rays, paraxial beams, and the adiabatic transform are still useful in a weakly range-dependent medium. When the medium does not have a preferential direction, the local plane wave spectra, such as asymptotic rays and paraxial beams, may remain useful.

B. Scattering Operators

If the scatterer or aperture is small, numerical methods such as method of moments, boundary elements and finite elements are good candidates to describe the coupling or scattering process. Both boundary elements and finite elements are discrete coordinate techniques, but they have complementary properties. The finite element method has the advantages that it can be applied to nonlinear and/or inhomogeneous media easily, and its coefficient matrices are sparse, which may be arranged to be banded, symmetric and diagonally dominant. The main disadvantage is that the unknowns must be of interest in the whole computing region. On the other hand, the boundary element method has the advantage that the unknowns can be solved only at some boundaries which may be far apart. It can not be employed to analyze nonlinear and/or inhomogeneous media easily. It also yields full coefficient matrices. A hybrid combination of these two methods have been proposed to

solve various problems. Here the hybrid boundary-finite elements are employed as a local operator to analyze wave scattering by inhomogeneous scatterers embedded in a global environment. The finite element method is employed to formulate the interior response of scatterers, and boundary element method to model the interaction among scatterers and the coupling between the interior and exterior of the scatterers. We also use the moment method as a local operator to analyze wave coupling through an aperture on one of the two walls of a waveguide. Note that the moment method is a weighted residue algorithm. If applied to a boundary, it is equivalent to the boundary element method when pulse expansion and weighting functions are employed. Similarly, if applied to a region, it is equivalent to the finite element method when small local elements are employed as expansion functions.

C. Combination of Global Propagators and Local Scattering Operators

By imposing the boundary conditions on the surface of a scatterer, the exterior propagator and interior operator will be integrated together. One way of doing so is to formulate the problem in terms of integral equations by invoking Green's theorem. By expressing the unknown field distributions along the scattering surface in terms of appropriate basis functions, these integral equations are then discretized and reduced to algebraic equations that are solved numerically. In the integral equations, the exterior Green's function is evaluated in terms of global propagators, and the interior response is modeled by local scattering operators.

3. PROGRESS TO DATE

In complicated structures, more and more methods with complementary properties are combined. At first, we had boundary elements-finite elements, rays-modes, boundary elements-modes, boundary elements-rays, boundary elements-spectral integral, etc. (Other local scattering operators such as T-matrix and moment method can be employed to replace the boundary element methods of the above list.) Then, we had boundary elements-finite elements-modes, boundary elements-rays-modes, and moment method-rays-modes, etc. Now we have boundary elements-finite elements-rays-modes. We have written up six journal papers and two proceeding papers. A listing of them is given in the publications.

4. FUTURE DIRECTIONS

Reliable and efficient algorithms for wave propagation and scattering in large and complicated structures are to be developed. Since no rigorous solution is available, a hybrid combination of various methods is a good way. To construct a hybrid scheme, the first step is to specify the applicable parameter regimes and to quantify the numerical efficiency and error of each individual method to be employed. These aspects are missing for many widely employed methods such as parabolic equation, beam shooting, local mode, etc. The second step is

to determine a combining strategy which indicates *a priori* where to employ a certain method and how to combine various methods together. This decision-making process has to be efficient, systematic, and physics oriented (otherwise, the hybrid method becomes a numbers game). The last step is to have an overall assessment of various aspects (such as applicable ranges, errors, efficiency, compatibility with other methods, etc) of the hybrid scheme. To make an algorithm robust and useful, this is a crucial step. In conclusion, to develop new hybrid schemes for unsolved problems and to make these new algorithms robust and efficient are the future directions.

5. PUBLICATIONS AND PAPERS

Journal Papers

Published

1. I.T. Lu, "Analysis of Acoustic Wave Scattering by Scatterers in Layered Media using the Hybrid Ray-Mode-(Boundary Integral Equation) Method," J. Acoust. Soc. Am., 86 (3), 1138-1142 (1989).

Accepted for Publication

2. B.L. Ma and I.T. Lu, "Electromagnetic Excitation of a Wire Enclosed in a Rectangular Cavity by a Plane Wave Incident on an Aperture," to appear in J. Electromagnetic Waves and Applications.
3. I.T. Lu and H.K. Jung, "A Hybrid (Boundary Elements)-(Finite Elements)-Ray-Mode Method for Wave Scattering by Inhomogeneous Scatterers in a Waveguide," to appear in J. Acoust. Soc. Am.
4. I.T. Lu, "A Hybrid Ray-Mode-(Boundary Element) Method," to appear in J. Electromagnetic Waves and Applications.
5. I.T. Lu and R. Olesen, "Analysis of Transmission Line Structures Suspended between Infinite Parallel Plates using a Numerically Efficient Image-Mode Green's Function," to appear in IEEE Trans. MTT.

Submitted for Publication

6. I.T. Lu and B.L. Ma, "A Hybrid Ray-Mode-Moment Method for Wave Scattering from an Aperture Coupled System," submitted to International Journal of Numerical Modeling: Electronic Networks, Devices and Fields.

Proceeding Papers

1. I.T. Lu and H.K. Jung, "Acoustic Wave Scattering by Multiple Scatters in a Waveguide," in Proceedings of the IMACS Symposium, Princeton University, March 1989.
2. E.C. Shang, Y.Y. Wang, H.Y. Chen and I.T. Lu, "Acoustic Source Localization in a Wedge-Shaped Shallow Water Waveguide," in Proceedings of the IMACS Symposium, Princeton University, March 1989.

E. OPTICAL SWITCHING AND SECOND HARMONIC GENERATION IN NONLINEAR THIN FILMS

Prof. B. Garetz

Unit EM9-5

1. OBJECTIVE(S)

The broad aims of this research program are to find new nonlinear optical materials, to adequately characterize their nonlinearities (both second and third order), and to use nonlinear materials to create new nonlinear optical devices.

We have set out to demonstrate experimentally a form of optical bistability that has been predicted theoretically by Professor K.M. Leung of the Polytechnic Physics Department. He has shown that the transmission and reflection of a TE electromagnetic wave from a nonlinear thin film on a linear substrate should exhibit optically bistable and multistable behavior, assuming the film has a Kerr-like nonlinearity [1]. This configuration is more complex than a simple nonlinear Fabry-Perot interferometer because the reflectivity at the linear/nonlinear interface is intensity dependent. Such experiments may have application to optical memory or laser hardening devices.

In addition, we are building a facility for the characterization of nonlinear optical materials, in particular, measuring second harmonic generation in Langmuir-Blodgett films, in cooperation with Dr. T. Skotheim at Brookhaven National Laboratory and Prof. Y. Okamoto of the Polytechnic Chemistry Department. The Langmuir-Blodgett technique provides a means for building up an ordered noncentrosymmetric array of organic molecules, which can then exhibit a bulk second order nonlinearity.

2. SUMMARY OF RECENT PROGRESS

We are setting up an experiment to study the transmission of a pulse of light from a Q-switched laser through a thin nonlinear polymer film on a silica substrate. We have obtained materials necessary for making thin nonlinear polymeric films, and are presently carrying out computer simulations to determine optimum experimental parameters. We have also set up an experimental facility for measuring second order optical nonlinearities in thin films (Langmuir-Blodgett) using second harmonic generation.

3. STATE OF THE ART AND PROGRESS DETAILS

A. Optical Switching

We have available to us, in the Weber Research Institute, facilities for spin coating thin films of organic and polymeric materials on glass substrates. We have obtained from Lifelines Technology samples of poly-4-BCMU polydiacetylene. This highly nonlinear material [nonresonant $X^{(3)} = 3 \times 10^{-11}$ esu at $1.06 \mu\text{m}$] is soluble in a number of organic solvents, unlike most polydiacetylenes, making it possible to cast films from solutions of the polymer [2,3]. The polymer has been characterized by NMR and FTIR spectroscopies to determine its purity.

The method chosen to observe the bistable behavior involves the transmission of a nanosecond optical pulse from a Q-switched Nd:YAG laser through the nonlinear film. Bistable behavior gives rise to differences in the reflection and transmission coefficients of the film during the rise versus during the fall of the pulse intensity. This generates pulse-shape asymmetries in the transmitted pulse, which can be observed on an oscilloscope [4]. We are setting up such an experimental facility using a Quanta-ray Nd:YAG laser.

With the cooperation of Professor Leung, we have developed a computer program that simulates the result of an experimental measurement. The program allows us to vary the experimental parameters (wavelength, film thickness, refractive indices of linear and nonlinear media, $X^{(3)}$ of nonlinear film, and angle of incidence), and to then see how the reflection coefficient varies with light intensity. We are presently performing simulations in order to determine the optimum conditions for observing optical switching. Not surprisingly, the largest effects calculated so far occur when the angle of incidence is very close to the critical angle of the linear/nonlinear interface. An example of such a simulation is shown in Fig. 1. When these studies are completed, we will proceed to fabricate film/substrate combinations in the appropriate geometry to try to observe the predicted phenomena.

B. Second Harmonic Generation

Preliminary tests have been performed on two Y-type Langmuir-Blodgett (LB) films of 4-[4-(N-n-dodecyl-N-methylamino)phenylazo]-3-nitrobenzoic acid (DPNA): one with 9 layers and the other with 21 layers, both deposited onto both sides of glass substrates. This particular material was previously investigated by Allen et al. [5]. These films were irradiated with $1.06 \mu\text{m}$ pulses from a Q-switched Nd:YAG laser, and second harmonic radiation at 532 nm was recorded as a function of angle of incidence. A typical experimental run is shown in Fig. 2. The peaks seen are not Maker fringes, but an interference pattern due to the interference between second harmonic generated at the front and back LB films.

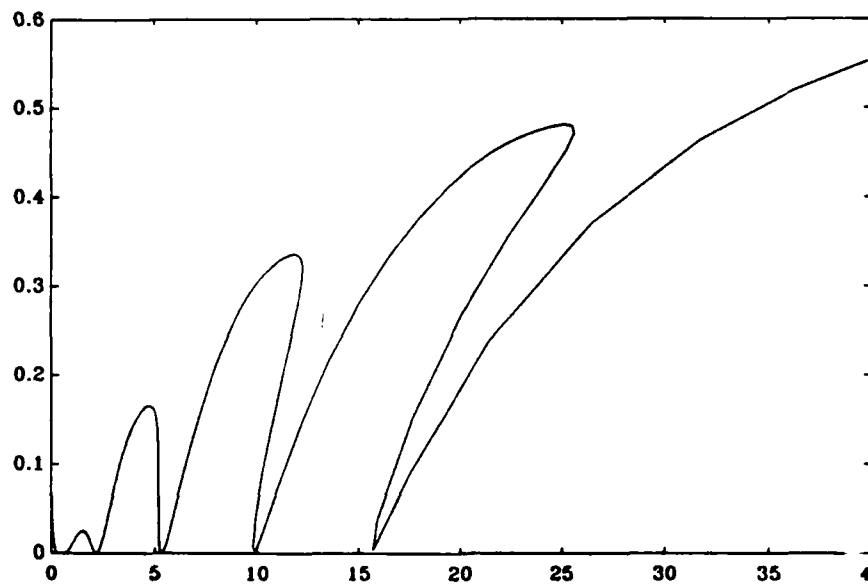


Fig. 1 Reflection coefficient vs. incident intensity for a particular experimental configuration.

SHG signal vs. Angle, 21 layer Y--type

LB film, DPNA

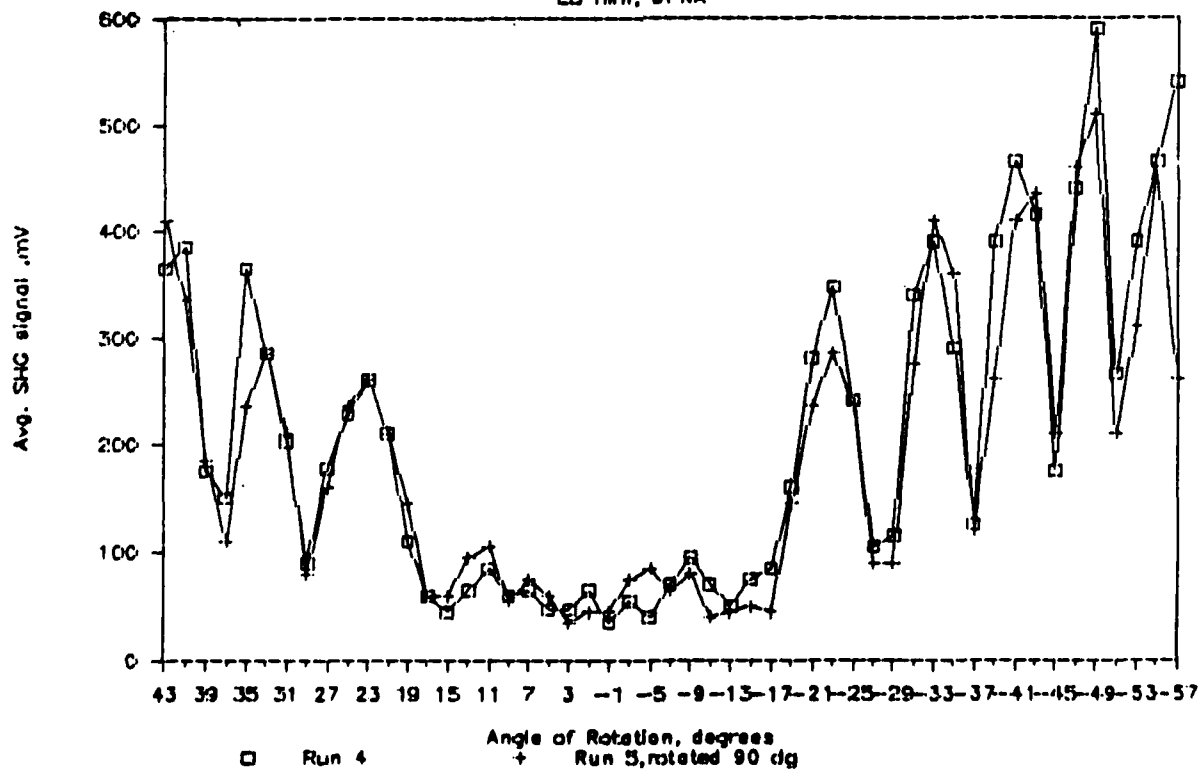


Fig. 2 Second harmonic signal vs. angle for Langmuir-Blodgett film.

4. REFERENCES

- [1] K.M. Leung, Phys. Rev. B**39**, 3590 (1989).
- [2] G. Berkovic, Y.R. Shen and P.N. Prasad, J. Chem. Phys. **87**, 1897 (1987).
- [3] W. Krug, E. Miao, M. Derstine and J. Valera, J. Opt. Soc. Am. B**6**, 726 (1989).
- [4] T. Bischofberger and Y.R. Shen, Phys. Rev. A**19**, 1169 (1979).
- [5] S. Allen, R.A. Haun, S.K. Gupta, P.F. Gordon, B.D. Bothwell, I. Ledoux, P. Vidakovic, J. Zyss, P. Robin, E. Chastaing and J.-C. Dubois, Proc. SPIE, Vol. 682, 97 (1986).

SECTION II
FIELD-PARTICLE INTERACTIONS IN MATTER (FP)

A. NONEQUILIBRIUM EM WAVE-COOPER PAIR INTERACTIONS IN HIGH T_c SUPERCONDUCTORS

Profs. E. Wolf, P. Riseborough and E. Kunhardt

Unit FP9-1

1. OBJECTIVE(S)

The cuprate superconductors with critical temperatures now as high as 125K are of great importance from basic and technical points of view. The discovery of these materials was a fortunate event, indeed, and the successful composition were not predicted by any theory. Neither the reason for the superiority of these materials, nor the mechanism by which exact pairing of their electrons [1] occurs is presently known. This circumstance hinders the search for even better materials. Thus, the mechanism by which superconductive pairing occurs in these materials remains of great importance. The objective of the present work is to determine the mechanism of pairing. It is likely that information relevant to applications will be discovered also in the course of the research.

The approach of the present research to gain information on the pairing mechanism of the cuprate superconductors is through study of the response of the superconductor to an external light pulse or other "pair-breaking" excitation, leading to a state of nonequilibrium. This novel approach is chosen because of our longstanding interest in nonequilibrium electronic phenomena, the known difficulty of standard techniques such as electron tunneling spectroscopy as applied to the cuprate superconductors, and because of interest in the nonequilibrium behavior and recovery times of the new materials from the point of view of potential applications. Further, our approach is a combined experimental and theoretical approach.

The response of a conventional superconductor to light of quantum energy $h\nu > 2\Delta$, with Δ the superconductor gap parameter, is well known to be breaking of pairs into distinct electron-like and hole-like quasiparticles, in concentrations in excess of their equilibrium values, which are set to the first approximation by the Boltzmann factor $\exp(-\Delta/kT)$. The presence of these internally excited particles (in addition to the superfluid pairs) may have two consequences. At sufficiently high density, the system will revert to the normal state. Below this critical density, the gap parameter of the superconductor will be slightly depressed, not materially affecting the superfluid behavior.

In this latter case, the excess quasiparticles may be detected by a biased quasiparticle tunnel junction which will collect quasiparticles and not collect pairs. The corresponding nonequilibrium voltage (a shift of the quasifermi level of quasiparticles from the chemical potential describing the pairs) can be measured on a tunnel junction [2] or on a normal metal contact to the

superconductor [3]. An additional indication of excess quasiparticles is dissipation induced by electromagnetic fields, which enter the superconductor to the penetration depths, and cause dissipative motion of the quasiparticles. Microwave measurements of the surface resistance reveal this effect.

The rate at which such excess quasiparticle populations decay in conventional superconductors (electron pairing by exchange of virtual phonons) is set by electron-hole recombination, emitting phonons to conserve energy and momentum and is well known [4]. Thus, a measurement of the recombination time in the new materials which yielded a much shorter time could be interpreted as an indication that a different collective mode of the system than the phonon interacts strongly with the electron and might be the cause also of the pairing. A second consequence of electronphonon coupling in the conventional case is that superconductivity depressed, i.e., pairs are broken, if the superconductor is subjected to a flux of phonons. By analogy, if say the new superconductor achieved pairing by exchange of excitons, then shining light known to create excitons onto the superconductor would also be expected to cause strong pairbreaking. By measuring the excess number of quasiparticles with a tunnel junction, and providing a photon flux of variable energy, it would be possible to test the importance of the exciton mechanism.

2. PROGRESS REPORT AND SUMMARY OF RECENT RESULTS

In this project, Prof. Wolf's group initially undertook growing superconductor films as well as designing the methods for detecting the internal nonequilibrium of the superconductor; Prof. Kunhardt's group is concerned with the pulse laser excitation and transient recording methods; and Prof. Riseborough's group generates theory relating to the general topic. Work in Wolf's group toward fabricating thin film samples of the $\text{RBa}_2\text{Cu}_3\text{O}_{7-x}$ compounds, where R is Dy and Sm, by thermal coevaporation of R, BaF_2 , and Cu terminated due to the loss of a graduate student and a technician. Films of superconductors have since been sought from the group of W.C. Wang, associated with the Weber Research Institute. These films to date have been polycrystalline as produced by single target sputtering onto room temperature LiNbO_3 , postannealed in oxygen, with rough surfaces. Masks have been drawn and fabricated to pattern the films into lines of widths between 6 and 2 micrometers, and several samples of these narrow lines have been successfully prepared. Due to the roughness of the films, little progress has been made in fabricating tunnel junctions on them. Progress in making microcontacts to these films has been made and will be discussed in Section 3, below. In view of the drawbacks of the present films, Wolf's group has grown single crystals of $\text{Bi}_2\text{Sr}_2\text{CaCu}_2\text{O}_8$ and, separately, a decision has been made to acquire an in-house capability for preparing laser ablated films. Work with the single crystals will be discussed in Section 3, below. The commercial helium refrigerator, capable of reaching 10K with optical windows and fast electrical and microwave coaxial line access, has been installed and is in use for measuring the transition

temperature of single crystal and thin film specimens. In Kunhardt's group, the picosecond laser system has been running, awaiting samples for study. In addition the decision has been made to purchase a new femtosecond pulse laser system, which can be used on this project. On the theoretical side, Prof. Riseborough's group has followed closely our experimental progress, as well as relevant experimental work elsewhere. In particular, the results of nonequilibrium excitation of cuprate superconductors by light of energy h exceeding the work function ϕ (Angle Resolved Photo-Electron Spectroscopy, ARPES) have been analyzed by Prof. Riseborough, and are discussed below.

3. STATE OF THE ART

A. Theory of High Energy Photoemission

Recently, the high energy optical response of high temperature superconductors has been measured by C. Olson, A.J. Arko and co-workers [5]. These investigators have used the technique of angle resolved photo-electron emission. In these measurements, a high energy photon interacts with an individual electron and is absorbed. Energy conservation dictates that the electron is excited and if the energy is sufficiently high it will leave the crystal, whereupon the photo-emitted electron may be detected, and have its energy and the direction of its momentum analyzed. The intensity of the flux of emitted electrons does, together with the principal of conservation of energy, lead directly to the determination of the spectrum for one electron removal processes in the solid. This excitation spectrum is not directly related to the density of the eigenvalues obtained in the usual local density function approximation used in electronic structure calculations, as the experimentally determined spectrum does contain the full effects of the correlations induced by electron-electron interactions. Prior measurements of the photoemission spectra have revealed that this discrepancy is unusually large in the high T_c materials. The electronic spectrum in the vicinity of the fermi-level is much reduced from the values obtained from L.D.A. electronic structure calculations [5,6]. This has been interpreted as suggesting [7] that the electron bands are split into two parts, by the effects of the repulsive inter-electron interaction such as to minimize the occupancy of the local Wannier orbitals on one atom, by more than one electron. That is the electronic band structure would be subjected to a Mott-Hubbard band splitting, such as is associated with the creation of a Slater antiferromagnet. This interpretation would lead to a gap in the excitation spectrum at the fermi-level, and result in an insulating state. Although the electronic resistivity of the normal state is high, it does show an approximately linear increase in resistivity with increasing temperature [8], and is thus not typical of the variation expected for such many-body insulators, but is more characteristic of a metal. The extremely anomalous properties of the normal state of the high temperature superconductors has caused Anderson to suggest that this is actually a new state of matter [9], and has stimulated the development of the theory [10] of the resonating valence bond state. The

existence and the properties of such a state are, at present, the subject of considerable controversy. In particular, it has been suggested that such materials do not have a conventional fermi-surface which would be marked by a discontinuity in the number of electrons as a function of wave vector [11] k , which could be directly determined by Compton scattering experiments. Varma [12] has suggested that the expected discontinuity vanishes for the high temperature superconductors. Anderson [13] has suggested that the resonating valence bond state would be characterized by a singularity in the one electron excitation spectrum at threshold, for wave vectors close to k_F as well as $3k_F$. An alternative picture of these materials, is the spin-bag approach pioneered by Schrieffer and co-workers [14]. Recently, Kampf and Schrieffer [15] have developed a theory of the electronic structure of high temperature superconductors, based on a model calculation that can be characterized as a fermi-liquid in which the inter electron interactions are close to driving the systems unstable to antiferromagnetic state. This picture is similar, in several respects, to a theory [16] concerning the photoemission spectra of strongly interacting, highly correlated, heavy fermion materials close to an instability to a localized state.

The advent of high intensity light sources has made it possible to improve the experimental resolution near the fermi level, to such an extent that these predictions may be tested. In particular, the experimental findings [5] showed that in the normal state, the angle resolved photoemission showed a sharp, asymmetrical peak close to the fermi level, at k_F . Furthermore, for k far from the fermi surface this peak washes out and joins onto the incoherent background due to multi-electron excitation processes. At low temperatures, the fermi-surface properties are no longer discerned due to the opening up of a superconducting gap or pseudo-gap in the density of states which is accompanied by a B.C.S. like piling up of the superconducting density of states at the edges of the gap [17,18].

It has been claimed, by Anderson [13], that the normal state angle resolved photoemission can *not* be described in terms of a conventional Landau fermi-liquid description. This claim is substantial and is contrary to the interpretation made by the experimental group [5], and so has stimulated [19] us to examine this point in greater detail.

Anderson's claims concerning the interpretation of angle resolved photoemission data, in terms of fermi-liquid are threefold:

1. Conventional Landau fermi-liquid theory will not produce a sharp and narrow asymmetric peak for k values located on the fermi-surface. Furthermore, if a peak does exist in the spectrum near the fermi-surface the spectra should show the fermi-surface discontinuity.
2. For k values off the fermi-surface, the experimental spectra vary linearly with the binding energies, as measured from the fermi-surface, whereas the Landau fermi-liquid theory for a three-dimensional metal would indicate a

quadratic dependent background.

3. The higher energy portions of the angle resolved photoemission form a constant k independent background.

These claims are based on the $T=0$ properties of the one-electron Green's function $G(k, k'; \omega)$, found from fermi-liquid theory. The angle resolved photoemission spectrum can be expressed [18,19] as

$$1/\pi \text{Im} G(k, k; \omega)$$

and the diagonal Green's function $G(k, k; \omega)$ can be expressed in terms of the irreducible self-energy, $\Sigma(k, \omega)$, via Dyson's equation

$$G(k, k; \omega) = \left[\omega - e(k) + \mu - \Sigma(k; \omega) \right]^{-1}$$

For a Landau fermi-liquid [20], the fermi surface is defined by

$$\mu = e(k_f) + \text{Re } \Sigma(k_f; 0)$$

and from Luttinger's theorem [20] the imaginary part vanishes quadratically with energy measured from the fermi surface,

$$\text{Im } \Sigma(k; \omega) \propto \omega^2$$

For energies and wave vectors close to the fermi surface, the real part of the self-energy can be expanded so that the denominator of the Green's function becomes

$$\omega \left[1 - d/d\omega \text{Re} \Sigma(k_f; \omega) \right] - (k - k_f) \cdot d/dk \left[e(k) + \Sigma(k; 0) \right]_{k_f} \\ + i \text{Im } \Sigma(k; \omega)$$

The factor multiplying ω is just the usual quasi-particle mass renormalization factor Z . If the k dependence of the self-energy can be neglected, then exactly on the fermi-surface the spectrum would be given by a Lorentzian of the form

$$1/\pi \left\{ \text{Im} \Sigma(k_f; \omega) / \omega^2 \right\} \left[\left(Z^2 + (\text{Im} \Sigma(k_f; \omega) / \omega)^2 \right)^{-1} \right]$$

where Z is the quasi-particle mass enhancement factor. Therefore, Anderson's claims are indeed correct. The Landau fermi-liquid theory would indeed predict a Lorentzian line shape, with a discontinuity at the fermi-surface due to the fermi-distribution function. However, that discontinuity is of order $1/Z^2$ and would be small for strongly enhanced systems, furthermore the discontinuous behavior is only present if k lies exactly on the fermi-surface. This latter condition is extremely difficult to ensure experimentally, and presumably in the experimentally determined data the two limits are not taken in the order implied in the above discussion. For k values only slightly different from k_f the $T=0$ spectrum will vanish at the fermi-energy quadratically with ω , thereby completely eliminating the small discontinuity

expected. This indeed would lead to an asymmetric line shape near the fermi-energy, which is narrow due to the almost vanishing of the self-energy. For k far removed from the fermi-surface k_f , the peak in the spectrum becomes more rapidly broadened and suppressed. Again, Landau fermi-liquid theory does predict that the spectrum would vanish quadratically with ω as it approaches the fermi-energy, due to the vanishing of $\text{Im } \Sigma(k;\omega)$, as Anderson [13] suggests. However, for highly enhanced fermi-liquids this region of ω^2 variation for larger energies. This linear behavior of the imaginary part of the self energy is found in the non-perturbative calculations of Doniach and Engelsbert [21], Lederer and Mills [22] etc. The results of reference [12] show that the extent of the approximate linear variation increase as Z increases. As Varma [12] noted, many of the low temperature properties of high T_c superconductors are consistent with extremely large or divergent values of Z and a concomitant linear variation of $\text{Im } \Sigma(k;\omega)$. Qualitatively, this extreme limit or, marginal fermi-liquid description does reproduce the linear variation observed in the photoemission experiments, noted by Anderson [13]. It also does explain the approximately linear variation found in the normal state resistivity [8], the low temperature T^2 term being either eliminated by the intervening superconducting transition or in the samples where the superconductivity is suppressed, the large enhancement factor Z is associated with the narrowness of the T^2 regime and may be too small to be observed in the experiments. Finally, the experimentally determined background was not well characterized, and as previously mentioned does not merely represent single electron processes but involves secondary electrons created in multi-electron-hole production processes, that is, processes involving multiple scattering. These secondary processes do yield a large contribution to the background which is k independent and which was not subtracted from the published data. The constancy of the background, as a function of k , can be interpreted as indicating that it is almost all due to these types of processes.

In view of the above qualitative arguments we have applied [19] a quantitative non-perturbative $1/N$ technique [16] to the calculation of the zero temperature limit of the photoemission spectrum. It did prove necessary to extrapolate the results to the regime of large N , in order to obtain the required large values of Z . The results found by this method [19] are in agreement with the expectations outlined above. In summary, it has been found that the spectra of high energy photo-emitted electrons from the high temperature superconductors can be interpreted in terms of a Landau fermi-liquid theory which is characterized by a large quasi-particle mass enhancement factor Z , thereby having an extremely small window around the fermi energy, in which the spectral response is characterized by fermi-liquid behavior. For energies further from the fermi-level, the response is characterized by a quasi-particle lifetime which varies approximately inversely linearly with the binding energy. This is roughly in accord with Varma's [12] observations about the properties of high temperature superconductors. However, the question as to whether Z^{-2} actually diverges to zero or is merely very small, is not resolved by the

presently available photoemission data.

B. Experimental

Optically generated quasiparticles can be detected by use of a biased quasiparticle tunnel junction, and nonequilibrium potential differences between pairs and quasiparticles can be detected using such junctions or, in practice, by normal metal (non-tunneling) contacts [3]. Since little progress has been achieved toward fabricating reliable quasiparticle junctions on the cuprate superconductors, especially those with rough surfaces, our effort has been directed toward (a) the growth of single crystals, and (b) the use of metal microcontacts of gold or silver. In the latter case, one can also get a measure of the energy gap of the material [23].

i. *Single Crystal Growth*

Single crystals of $\text{Bi}_2\text{Sr}_2\text{CaCu}_2\text{O}_8$ (BSCCO) have been prepared following the method of Mitzi, et al. [24]. A mixture of oxides containing about 20% excess BiO is placed in a covered Coors alumina crucible and heated in air to 930°C . The geometry is chosen to provide a horizontal temperature gradient across the surface of the melt. After soaking for 2 hours, cooling at 0.7°C per hour continues to 720°C , followed by furnace coolings. Single crystals showing perfect facets of dimensions several millimeters are evident at the surface of the deposit. Resistive transitions are centered at 92K, and the c-axis normal orientation of the crystalline facets is verified by the x-ray diffractometer trace shown in Fig. 1.

In Fig. 1 only prominent OOL peaks, in agreement with the 2212 BSCCO structure [25] are seen with the x-ray scattering vector coincident with the surface normal. Prior to this, a few small single crystals of 85K T_c had been obtained courtesy of Dr. Z. Igbal, Allied-Signal, Inc., Morristown, NJ.

ii. *Tunneling Spectra of Single Crystals*

The dI/dV spectrum obtained between a gold tip and a small single crystal of 85K BSCCO is shown in Fig. 2. This spectrum was obtained using a cryogenic scanning tunneling microscope, immersed in liquid helium, which stabilized an effective tunneling barrier between the Au and BSCCO.

The software used to control the microscope and process the data have been described by Rong [26]. Figure 2 presents a tunneling dI/dV spectrum, interpretable as a smeared BCS-like density of quasiparticle excitations consistent with a large effective gap parameter of about 35 mV. These results will be more extensively reported elsewhere [27,28].

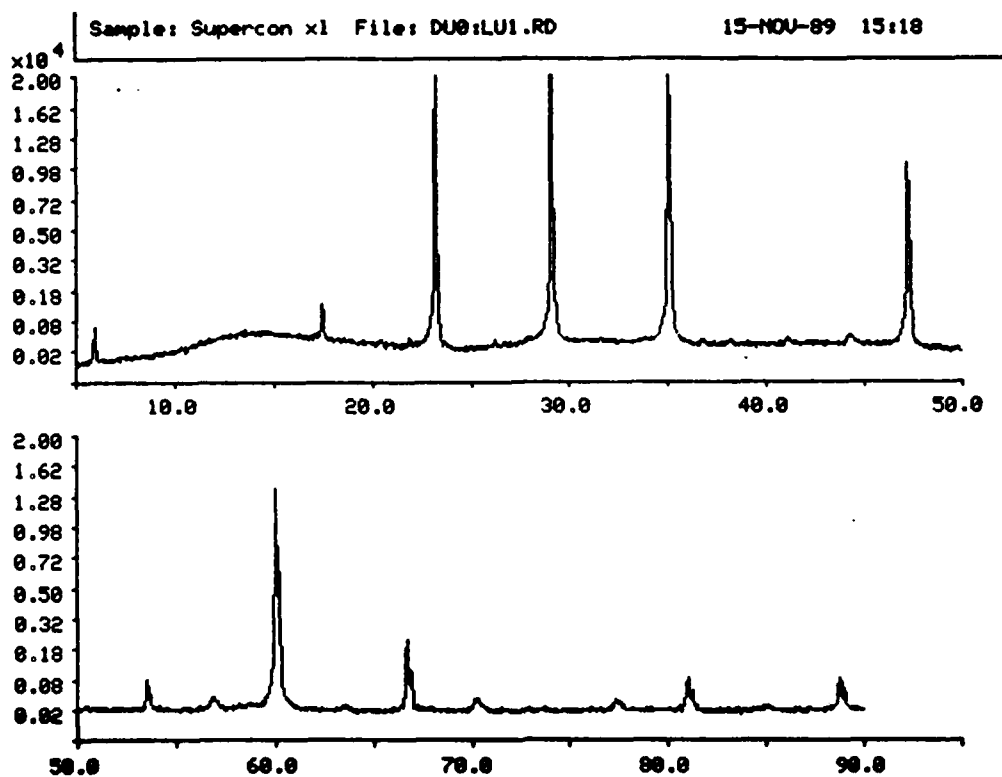


Fig. 1 Diffractometer traces of $\text{Bi}_2\text{Sr}_2\text{CaCu}_2\text{O}_8$ crystal using copper K radiation. The prominent 00L reflections originate from such planes parallel to the large facets on the surface of the crystal.

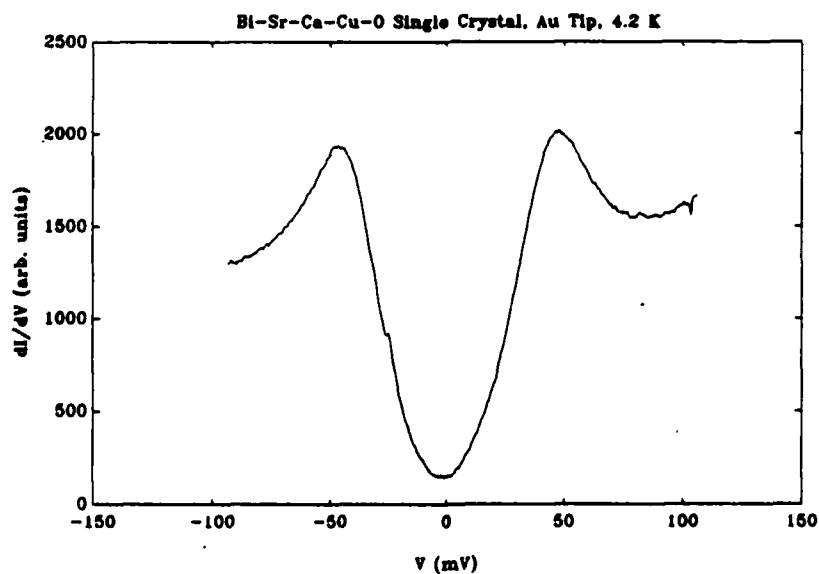


Fig. 2 Tunneling spectrum obtained in cryogenic scanning tunneling microscope at 4.2K using Au tip.

iii. Point Contact Spectra of Single Crystals

A different I-V behavior is obtained when a Au tip is in direct contact with the BSCCO surface. These curves are approximately linear in a range of 16 mV centered at $V=0$, and fall to approximately linear behavior of half the slope beyond this value. This behavior in microcontacts between normal metals and superconductors can be interpreted in terms of Andreev reflection of normal electrons into holes, with a pair being generated within the superconductor [23]. This process, which operates only for $eV < \Delta$, doubles the total current in that range. Thus, one would identify the gap value from such a curve as the voltage at which the slope change occurs, i.e., $\Delta=8\text{meV}$ in the case mentioned.

The difference between this estimate and that obtained from the tunneling spectrum of Fig. 2 may arise from the expected anisotropy of the BSCCO crystals, if the tunneling direction were parallel to the a,b plane of the material, and the point contact orientation were perpendicular to those planes. It is also expected, in the point contact case, with strong overlap of electrons between the materials through the contact, that the local gap value in the superconductor will be depressed.

Spectra giving evidence of Andreev reflection, but showing less distinct changes of slope of the I-V curve, have been obtained also on thin film specimens recently obtained, courtesy of Prof. Wang.

4. REFERENCES

- [1] C. Gough, et al., Nature, **326** 30 (1987).
- [2] J. Clarke, Phys. Rev. Lett. **28** 1363 (1972).
- [3] G.J. Dolan and L.D. Jackel, Phys. Rev. Lett., **39** 1628 (1977).
- [4] S.B. Kaplan, C.C. Chi, D.N. Langenberg, J.J. Chang, S. Jafarey and D.J. Scalapino, Phys. Rev., **B14** 4854 (1976).
- [5] C. Olson and A.J. Arko, Phys. Rev. Lett. (submitted).
- [6] S. Massida, J. Yu and A.J. Freeman, Phys. Lett. A, **122** 198 (1987).
- [7] T. Nakano, K. Okada and A. Kotani, J. Phys. Soc. Japan, **57** 655 (1988).
- [8] M. Gurvitch and A.T. Flory, Phys. Rev. Lett., **59** 1337 (1987).
- [9] P.W. Anderson, Science, **235** 1196 (1987).
- [10] P.W. Anderson, G. Baskaran, Z. Ahou and T. Hsu, Phys. Rev. Lett., **58** 2790 (1987).
- [11] P.W. Anderson, Physic B (in press).
- [12] C.M. Varma, Preprint.

- [13] P.W. Anderson, Preprint (N.Y.A.S.).
- [14] J.R. Schreiffer, X.G. Wen and S.C. Zhang, Phys. Rev. Lett., **60** 944 (1988).
Phys. Rev., **B39** 11663 (1989).
- [15] A. Kampf and J.R. Schreiffer, Physica B (in press) submitted to Phys. Rev. B.
- [16] Peter S. Riseborough, Phys. Rev. B., **40** 8131 (1989). For the extension to finite temperature see J. Appl. Phys. (in press).
- [17] A.J. Arko et al., Phys. Rev. B submitted.
- [18] Y. Baer, Phys. Rev. B submitted.
- [19] H. Kim and P.S. Riseborough (in preparation).
- [20] J.M. Luttinger, Phys. Rev., **119** 1153 (1960).
Phys. Rev., **121** 942 (1961).
- [21] A.B. Kaiser and S. Doniach, J. Magnetism, **1** 11 (1970).
- [22] P. Lederer and D.L. Mills, Phys. Rev., **165** 837 (1968).
- [23] P.C. van Son, H. van Kempen and P. Wyder, Phys. Rev. Lett., **59** 2226 (1987).
- [24] D.B. Mitzi, L.W. Lombardo, A. Kapitulnik, S.S. Laderman and R.D. Jacowitz, Phys. Rev. B. (in press).
- [25] X.Z. Whang, K. Donnelly, T. Bakas and J.M.D. Coey, Solid State Commun., **69** 829 (1989).
- [26] Z. Rong, Technical Report " 'C' Programs for Scanning Tunneling Spectroscopy Data Acquisition," Polytechnic University, Physics Dept., February 1989.
- [27] B. Susla, Z. Rong, S. Meepagala, G. Hunter, Z. Igbal and E.L. Wolf, "Low Temperature STM-Spectroscopy of Bi-Sr-Ca-Cu-O Single Crystals and Sintered Material," presented at International Conference Materials and Mechanisms of Superconductivity: High Temperature Superconductors, Stanford University, July 23-28, 1989.
- [28] B. Susla, Z. Rong, G. Hunter, Z. Igbal and E.L. Wolf, "Cryogenic STM Superconductive and Coulomb Blockade Tunneling Spectroscopy of Bi-Sr-Ca-Cu-O Materials," in International Conference on High- T_c Thin Films and Single Crystals, Ustron, Poland, September 30 - October 4, 1989 (to be published).